

Renormalization group approach to interacting fermion systems in the two-particle-irreducible formalism

N. Dupuis

*Department of Mathematics, Imperial College, 180 Queen's Gate, London SW7 2AZ, UK and
Laboratoire de Physique des Solides, CNRS UMR 8502, Université Paris-Sud, 91405 Orsay, France*

(Dated: June 21, 2005)

We describe a new formulation of the functional renormalization group (RG) for interacting fermions within a Wilsonian momentum-shell approach. We show that the Luttinger-Ward functional is invariant under the RG transformation, and derive the infinite hierarchy of flow equations satisfied by the two-particle-irreducible (2PI) vertices. In the one-loop approximation, this hierarchy reduces to two equations that determine the self-energy and the 2PI two-particle vertex $\Phi^{(2)}$. Susceptibilities are calculated from the Bethe-Salpeter equation that relates them to $\Phi^{(2)}$. While the one-loop approximation breaks down at low energy in one-dimensional systems (for reasons that we discuss), it reproduces the exact results both in the normal and ordered phases in single-channel (i.e. mean-field) theories, as shown on the example of BCS theory. The possibility to continue the RG flow into broken-symmetry phases is an essential feature of the 2PI RG scheme and is due to the fact that the 2PI two-particle vertex, contrary to its 1PI counterpart, is not singular at a phase transition. Moreover, the normal phase RG equations can be directly used to derive the Ginzburg-Landau expansion of the thermodynamic potential near a phase transition. We discuss the implementation of the 2PI RG scheme to interacting fermion systems beyond the examples (one-dimensional systems and BCS superconductors) considered in this paper.

PACS numbers: 05.10.Cc, 05.30.Fk, 71.10.-w

I. INTRODUCTION

The two-particle-irreducible (2PI) formalism^{1,2,3,4,5} was first introduced in condensed-matter physics as a means to systematically set up self-consistent approximations that satisfy conservation laws. It can be cast in a variational framework where the thermodynamic potential Γ is expressed as a functional of the single-particle Green function.⁶ Γ is essentially determined by the Luttinger-Ward (LW) functional Φ ,¹ given by the sum of the 2PI Feynman diagrams. Φ is also the generating functional of the self-energy and higher-order 2PI vertices. The so-called Φ -derivable approximations are based on truncations of the diagrammatic expansion of Φ that retain only a finite number or a sub-series of diagrams. They are thermodynamically consistent and satisfy conservation laws.^{3,7} While most applications of the 2PI formalism to interacting fermion systems have been limited to the Hartree-Fock level, recent developments, motivated by the physics of high-temperature superconductors, have incorporated exchange of spin fluctuations within the Hubbard model.^{8,9,10} Following general ideas put forward by Wetterich,¹¹ the aim of this paper is to discuss a 2PI formulation of the renormalization group (RG) approach to interacting fermion systems.

The RG has proven a powerful approach for studying low-dimensional fermion systems, providing a systematic and unbiased method to study competing instabilities in the weak-coupling limit (Refs. 12-40). One of its main successes has been to explain how unconventional superconductivity can occur at low temperature in systems like organic conductors^{12,13,14,15,16} or high-temperature superconductors^{20,21,22,23,25} where the dom-

inant electron-electron interactions are expected to be repulsive and favor antiferromagnetism. Although the RG can be implemented in different ways, most approaches rely on the so-called one-particle-irreducible (1PI) RG scheme or variants thereof.^{23,25,41} The 1PI RG scheme is based on an exact RG equation for the generating functional of 1PI vertices. The existence of a Fermi surface implies that the interaction amplitudes strongly depend on the momenta of the interacting fermions, which leads to functional RG equations for the 1PI vertices. For this reason, most RG calculations in fermion systems have been limited to one-loop order and are thus restricted to the weak-coupling limit. Another severe limitation of the method comes from the difficulty to access broken-symmetry phases. Long-range order is signaled by a diverging flow of certain 1PI vertices and susceptibilities at a critical energy or temperature scale, below which the RG equations cannot be continued. It has been proposed to circumvent this difficulty by introducing an infinitesimally small symmetry-breaking component in the initial condition of the RG equations,²⁸ or combining the RG technique with a mean-field approximation at low energy.^{42,43} Alternatively, one can introduce a partial bosonization of the action yielding a description in terms of both fermionic and collective Hubbard-Stratonovich fields.^{11,32,38,39} It will be interesting to further explore the applicability of these new RG schemes in various models.

The main purpose of this paper is to show that broken-symmetry phases can be studied with a RG scheme where the basic quantities are the 2PI vertices rather than their 1PI counterparts. To understand this issue in simple terms, let us consider the 1PI two-particle vertex in the spin singlet particle-particle channel obtained by sum-

ming the bubble diagrams (random-phase approximation (RPA)),

$$\gamma = \frac{\gamma_0}{1 + l\gamma_0}, \quad (1)$$

where $l \sim \ln(\Lambda_0/\Lambda)$ comes from the non-interacting particle-particle propagator. Λ_0 is a high-energy cutoff (e.g. the bandwidth), Λ an infrared cutoff which can be identified with the temperature, and γ_0 the bare (dimensionless) interaction. In the RG framework, γ can be interpreted either as the 1PI vertex of a theory with infrared cutoff Λ or as the effective interaction of the Wilsonian action with ultraviolet cutoff Λ .⁴⁴ Eq. (1) becomes a differential equation (see e.g. Ref. 45),

$$\frac{d\gamma}{dl} = -\gamma^2. \quad (2)$$

For an attractive interaction $\gamma_0 < 0$, a divergence occurs at the energy (or temperature) scale $\Lambda_c = \Lambda_0 \exp(1/\gamma_0)$, signaling the formation of Cooper pairs and the appearance of long-range superconducting order. In the BCS (mean-field) theory, this divergence is cured below Λ_c by the presence of a finite gap in the fermion excitation spectrum. However, in the 1PI RG scheme, it prevents the flow to be straightforwardly²⁸ continued into the broken-symmetry phase.

Let us now reconsider Eq. (1) from a different point of view. This equation can be seen as a Bethe-Salpeter equation in the particle-particle channel with the bare interaction γ_0 as the 2PI vertex $\Phi^{(2)}$ (the reason for this notation will become clear in Sec. II). Only the non-interacting particle-particle propagator $\sim l \sim \ln(\Lambda/\Lambda_0)$ is scale dependent in Eq. (1), while the 2PI vertex $\Phi^{(2)}$ is invariant under the RG transformation,

$$\frac{d\Phi^{(2)}}{dl} = 0. \quad (3)$$

Within the BCS theory, the 2PI vertex $\Phi^{(2)}$ is therefore not sensitive to the transition into the superconducting phase. The appearance of long-range order is expected to induce an anomalous (i.e. symmetry violating) self-energy below Λ_c . In more complicated cases, where several types of fluctuations may compete together, we cannot exclude the appearance of singularities in the 2PI vertices. For instance, in a conductor close to an antiferromagnetic instability, singularities in the particle-particle channel (i.e. in the particle-particle component of $\Phi^{(2)}$) may be induced by nearly divergent spin fluctuations. We shall discuss this point in the concluding section and explain how these singularities can be controlled by a proper parameterization of the vertex. All these considerations suggest to use a RG scheme where the basic objects are the 2PI vertices.

The outline of the paper is as follows. In Sec. II A, we briefly recapitulate the 2PI formalism. By means of a Legendre transformation, we express the thermodynamic potential (grand potential) as a functional $\Gamma[G]$ of the

Green function; we then define the LW functional $\Phi[G]$ and the 2PI vertices $\Phi^{(n)}$. In Sec. II B, we describe the RG procedure. We derive the differential equation satisfied by the thermodynamic potential and show that the LW functional is invariant under the RG transformation. We then deduce the infinite hierarchy of flow equations satisfied by the 2PI vertices. A one-loop approximation is then introduced by truncating this hierarchy and approximating the 2PI three-particle vertex in terms of the 2PI two-particle vertex $\Phi^{(2)}$ (Sec. II C). We discuss the connection between the one-loop equations and their counterparts in the 1PI RG scheme. In Secs. II D and II E, we give explicit expressions of the one-loop flow equations in the normal phase and discuss the calculation of response functions. Some of the general results of Secs. II A-II E have been previously obtained by Wetterich,¹¹ sometimes in a slightly different formulation, with a few important differences that we shall mention. In Sec. II F, we show how the normal phase RG equations can be used to derive the Ginzburg-Landau expansion of the thermodynamic potential in the vicinity of a phase transition. This is achieved by considering the Legendre transform $F[\Sigma]$ of the LW functional $\Phi[G]$, which allows one to express the thermodynamic potential as a functional of the self-energy. The latter is then split into a normal part and an anomalous (i.e. symmetry violating) part which is to be determined by minimizing the thermodynamic potential. The last two sections are devoted to the application of the 2PI RG formalism to two different models. In Sec. III, we consider a three-dimensional fermion system with an attractive interaction. From the one-loop approximation restricted to the particle-particle channel, we rederive the main results of the BCS theory (gap equation, thermodynamic potential, and collective modes), thus showing the ability of the 2PI RG scheme to access broken-symmetry phases. We find that the 2PI two-particle vertex $\Phi^{(2)}$ is invariant under the RG transformation, while the flow equation for the self-energy yields the BCS gap equation. In Sec. IV, we study one-dimensional (1D) systems within the g-ology framework. At one-loop order, the 2PI scheme compares favorably to the RG scheme at high energy, but deteriorates at lower energy and eventually breaks down. We identify the reason for this failure and argue that the 2PI RG scheme can nevertheless be applied to realistic quasi-1D systems like the organic conductors of the Bechgaard salt family. The conclusion is devoted to a discussion of the implementation of the 2PI RG formalism beyond the examples considered in Secs. III and IV.

RG approaches in the 2PI formalism have also been discussed in high-energy physics in a field-theoretical framework (see, for instance, Refs. 46,47,48,49).

II. 2PI RG FORMALISM

A. Luttinger-Ward functional and 2PI vertices

We consider the partition function of a spin- $\frac{1}{2}$ fermion system in the presence of external sources,

$$Z[J] = \int \mathcal{D}[\psi] \exp\left\{-S[\psi] + \frac{1}{2}\psi^T J\psi\right\}, \quad (4)$$

where the action $S = S_0 + S_{\text{int}}$ is defined by

$$\begin{aligned} S_0[\psi] &= \frac{1}{2} \sum_{\alpha,\beta} \psi_\alpha C_{\alpha\beta}^{-1} \psi_\beta, \\ S_{\text{int}}[\psi] &= \frac{1}{4!} \sum_{\alpha_1,\alpha_2,\alpha_3,\alpha_4} V_{\alpha_1\alpha_2\alpha_3\alpha_4} \psi_{\alpha_1} \psi_{\alpha_2} \psi_{\alpha_3} \psi_{\alpha_4}, \end{aligned} \quad (5)$$

with $C_{\alpha\beta}$ the free propagator and $V_{\alpha_1\alpha_2\alpha_3\alpha_4}$ the totally antisymmetrized interaction vertex. $\frac{1}{2}\psi^T J\psi = \frac{1}{2} \sum_{\alpha,\beta} \psi_\alpha J_{\alpha\beta} \psi_\beta$ describes the coupling to the external bosonic sources $J_{\alpha\beta}$. The ψ_α 's are Grassmann variables and the collective index $\alpha \equiv (\mathbf{r}, \tau, \sigma, c)$ labels the position, imaginary time and spin projection along a given axis, as well as other possible internal degrees of freedom. $\sum_\alpha = \int_0^\beta d\tau \int d^d r \sum_{\sigma,c}$ where $\beta = 1/T$ is the inverse temperature and d the space dimension. $c = \pm$ is a charge index such that

$$\psi_\alpha = \begin{cases} \psi_\sigma(\mathbf{r}, \tau) & \text{if } c = -, \\ \psi_\sigma^*(\mathbf{r}, \tau) & \text{if } c = +. \end{cases} \quad (6)$$

Since the ψ 's anticommute, both $C_{\alpha\beta}$ and $J_{\alpha\beta}$ can be chosen to be antisymmetric functions: $C_{\alpha\beta} = -C_{\beta\alpha}$ and $J_{\alpha\beta} = -J_{\beta\alpha}$. In the following, we denote by

$$\gamma = \{\alpha, \beta\} \quad (7)$$

bosonic indices obtained from two fermionic indices α and β .

The single-particle Green function is given by the functional derivative of $W[J] = \ln Z[J]$,

$$G_\gamma = \langle \psi_\alpha \psi_\beta \rangle = \frac{\delta W[J]}{\delta J_\gamma}. \quad (8)$$

Note that the definition of G differs by a minus sign from the usual definition in condensed-matter physics. The Legendre transform of $W[J]$ is defined by

$$\Gamma[G] = -W[J] - \frac{1}{2} \text{Tr}(JG), \quad (9)$$

where $J \equiv J[G]$ is obtained by inverting Eq. (8). To keep the notations simple, we shall denote $J[G]$ by J in the following. Tr denotes the trace with respect to the fermionic indices, i.e. $\text{Tr}(JG) = \sum_{\alpha,\beta} J_{\alpha\beta} G_{\beta\alpha}$. $\Gamma[G]$ satisfies the ‘‘equation of motion’’

$$\frac{\delta \Gamma[G]}{\delta G_\gamma} = J_\gamma, \quad (10)$$

as can be easily verified by a direct calculation.⁵⁰ It is customary to write $\Gamma[G]$ as

$$\Gamma[G] = \frac{1}{2} \text{Tr} \ln G - \frac{1}{2} \text{Tr}(GC^{-1} - 1) + \Phi[G], \quad (11)$$

where the LW functional $\Phi[G]$ is the sum of 2PI vacuum fluctuation diagrams (or vacuum fluctuation skeleton diagrams), i.e. diagrams that cannot be separated into two disconnected pieces by cutting two lines.

By differentiating Eq. (10) with respect to the source J and using Eq. (8),⁵⁰ we obtain

$$\begin{aligned} (\Gamma^{(2)}W^{(2)})_{\gamma_1\gamma_2} &\equiv \frac{1}{2} \sum_{\gamma_3} \Gamma_{\gamma_1\gamma_3}^{(2)} W_{\gamma_3\gamma_2}^{(2)} \\ &= \delta_{\alpha_1,\alpha_2} \delta_{\beta_1,\beta_2} - \delta_{\alpha_1,\beta_2} \delta_{\beta_1,\alpha_2} \\ &\equiv I_{\gamma_1\gamma_2} \end{aligned} \quad (12)$$

where

$$\begin{aligned} \Gamma_{\gamma_1 \dots \gamma_n}^{(n)} &= \frac{\delta^{(n)} \Gamma[G]}{\delta G_{\gamma_1} \dots \delta G_{\gamma_n}}, \\ W_{\gamma_1 \dots \gamma_n}^{(n)} &= \frac{\delta^{(n)} W[J]}{\delta J_{\gamma_1} \dots \delta J_{\gamma_n}} \end{aligned} \quad (13)$$

are functionals of G . Eq. (12) defines a matrix multiplication with respect to the bosonic indices with I the unit matrix. Further relations between $\{W^{(n)}\}$ and $\{\Gamma^{(n)}\}$ can be obtained by taking higher-order derivatives of the equation of motion (10).

The 2PI vertices are defined by

$$\Phi_{\gamma_1 \dots \gamma_n}^{(n)} = \frac{\delta^{(n)} \Phi[G]}{\delta G_{\gamma_1} \dots \delta G_{\gamma_n}}. \quad (14)$$

To order V^m , $\Phi^{(n)}$ is represented by all 2PI diagrams with n external (bosonic) legs γ_i and $2m - n$ internal lines. These diagrams cannot be separated into two disconnected pieces by cutting two internal lines (considering every external leg $\gamma_i = \{\alpha_i, \beta_i\}$ as a connected piece). The 2PI vertices satisfy the symmetry properties

$$\begin{aligned} \Phi_{\gamma_1 \dots \{\alpha_i, \beta_i\} \dots \gamma_n}^{(n)} &= -\Phi_{\gamma_1 \dots \{\beta_i, \alpha_i\} \dots \gamma_n}^{(n)}, \\ \Phi_{\gamma_1 \dots \gamma_i \dots \gamma_j \dots \gamma_n}^{(n)} &= \Phi_{\gamma_1 \dots \gamma_j \dots \gamma_i \dots \gamma_n}^{(n)}. \end{aligned} \quad (15)$$

The equation of motion (10) can be rewritten as a Dyson equation

$$G_\gamma^{-1} = C_\gamma^{-1} - J_\gamma + \Sigma_\gamma, \quad (16)$$

with $\Sigma_\gamma = \Phi_\gamma^{(1)}$ the self-energy. Note that the diagrammatic interpretation of $\Phi[G]$ as the sum of 2PI vacuum fluctuation diagrams follows from Eq. (16) (see, for instance, Ref. 51). Similarly, the equation $\Gamma^{(2)}W^{(2)} = I$ can be recast in the form

$$\begin{aligned} W_{\gamma_1\gamma_2}^{(2)} &= G_{\alpha_1\beta_2} G_{\beta_1\alpha_2} - G_{\alpha_1\alpha_2} G_{\beta_1\beta_2} \\ &+ \frac{1}{2} \sum_{\gamma_3,\gamma_4} G_{\alpha_1\alpha_3} G_{\beta_1\beta_3} \Phi_{\gamma_3\gamma_4}^{(2)} W_{\gamma_4\gamma_2}^{(2)}. \end{aligned} \quad (17)$$

Eq. (17) is a Bethe-Salpeter equation relating the two-particle Green function $W^{(2)}$ to the 2PI vertex $\Phi^{(2)}$.

Equilibrium quantities are obtained for vanishing external sources ($J = 0$). The equilibrium Green function \bar{G} is determined by the stationary condition

$$\left. \frac{\delta \Gamma[G]}{\delta G_\gamma} \right|_{\bar{G}} = 0. \quad (18)$$

It can be expressed in terms of the self-energy $\bar{\Sigma} = \Sigma|_{\bar{G}} = \bar{\Phi}^{(1)}$,

$$\bar{G}_\gamma^{-1} = C_\gamma^{-1} + \bar{\Sigma}_\gamma. \quad (19)$$

The thermodynamic potential is given by $\Omega = -\beta^{-1} \ln Z[J = 0] = \beta^{-1} \Gamma[\bar{G}]$.

B. 2PI RG equations

We now take the free propagator C to depend on an infrared cutoff Λ which suppresses the low-energy degrees of freedom ($|\xi_{\mathbf{k}}| \lesssim \Lambda$),

$$C(\mathbf{k}, i\omega_n) = -\frac{\Theta_{\mathbf{k}}}{i\omega_n - \xi_{\mathbf{k}}}. \quad (20)$$

$C(\mathbf{k}, i\omega_n)$ is the Fourier transform of $C(\mathbf{r}, \tau, -; \mathbf{r}', \tau', +)$, which we assume to be spin-rotation invariant. $\xi_{\mathbf{k}} = \epsilon_{\mathbf{k}} - \mu$ is the dispersion of the free fermions (with μ the chemical potential), and ω_n a fermionic Matsubara frequency. $\Theta_{\mathbf{k}}$ is a cutoff function such that $\Theta_{\mathbf{k}}|_{\Lambda=0} = 1$ and $\Theta_{\mathbf{k}}|_{\Lambda=\Lambda_0} = 0$, where $\Lambda_0 = \max_{\mathbf{k}} |\xi_{\mathbf{k}}|$. Physical quantities are obtained for $\Lambda = 0$, when all degrees of freedom are included in the partition function. $W[J]$ and its Legendre transform $\Gamma[G]$ now depend on Λ and satisfy flow equations as the cutoff Λ is varied between Λ_0 and 0.

From the definition of $\Gamma[G]$ [Eq. (9)], we deduce

$$\begin{aligned} \frac{d}{dl} \Gamma[G] &= -\frac{\partial}{\partial l} W[J] - \frac{1}{2} \sum_\gamma \frac{dJ_\gamma}{dl} \frac{\delta W[J]}{\delta J_\gamma} - \frac{1}{2} \text{Tr} \left(\frac{dJ}{dl} G \right) \\ &= -\frac{\partial}{\partial l} W[J], \end{aligned} \quad (21)$$

where l can be either Λ or a function of Λ , e.g. $l = \ln(\Lambda_0/\Lambda)$. Recall that J depends on G via Eq. (8) and is therefore a function of l . $\partial W[J]/\partial l$ denotes the variation of $W[J] = \ln Z[J]$ which follows from the explicit Λ dependence of the propagator C ,

$$\begin{aligned} \frac{\partial}{\partial l} W[J] &= \frac{1}{Z[J]} \int \mathcal{D}[\psi] \left(-\frac{1}{2} \psi^T \dot{C}^{-1} \psi \right) e^{-S[\psi] + \frac{1}{2} \psi^T J \psi} \\ &= -\frac{1}{2} \sum_{\alpha, \beta} \dot{C}_{\alpha\beta}^{-1} \langle \psi_\alpha \psi_\beta \rangle \\ &= \frac{1}{2} \text{Tr}(\dot{C}^{-1} G), \end{aligned} \quad (22)$$

where the dot denotes a derivation with respect to l . Eqs. (21,22) imply

$$\frac{d}{dl} \Gamma[G] = -\frac{1}{2} \text{Tr}(\dot{C}^{-1} G), \quad (23)$$

and, using Eq. (11),

$$\frac{d}{dl} \Phi[G] = 0. \quad (24)$$

The LW functional is invariant under the RG transformation. It is therefore a ‘‘universal’’ functional independent of the free propagator C .⁵² This property has a simple diagrammatic interpretation. Being the sum of the 2PI graphs (with the internal lines corresponding to the variable G), $\Phi[G]$ depends on the interaction vertex V , but not on the non-interacting (Λ -dependent) propagator C .

The thermodynamic potential satisfies the RG equation

$$\begin{aligned} \dot{\Omega} &= \frac{1}{\beta} \frac{d}{dl} \left(\Gamma[G] \Big|_{\bar{G}} \right) \\ &= \frac{1}{\beta} \left(\frac{d}{dl} \Gamma[G] \right)_{\bar{G}} + \frac{1}{2\beta} \sum_\gamma \left. \frac{\delta \Gamma[G]}{\delta G_\gamma} \right|_{\bar{G}} \dot{\bar{G}}_\gamma \\ &= -\frac{1}{2\beta} \text{Tr}(\dot{C}^{-1} \bar{G}), \end{aligned} \quad (25)$$

where the last line is obtained using equations (23) and (18).

Since $\Phi[G]$ is invariant under the RG transformation, the flow of the 2PI vertices $\bar{\Phi}^{(n)} = \Phi^{(n)}|_{\bar{G}}$ is entirely due to the flow of \bar{G} ,

$$\begin{aligned} \dot{\bar{\Phi}}_{\gamma_1 \dots \gamma_n}^{(n)} &= \frac{d}{dl} \left(\left. \frac{\delta^{(n)} \Phi[G]}{\delta G_{\gamma_1} \dots \delta G_{\gamma_n}} \right|_{\bar{G}} \right) \\ &= \frac{1}{2} \sum_\gamma \left. \frac{\delta^{(n+1)} \Phi[G]}{\delta G_{\gamma_1} \dots \delta G_{\gamma_n} \delta G_\gamma} \right|_{\bar{G}} \frac{d}{dl} \bar{G}_\gamma \\ &= \frac{1}{2} \sum_\gamma \bar{\Phi}_{\gamma_1 \dots \gamma_n \gamma}^{(n+1)} \dot{\bar{G}}_\gamma. \end{aligned} \quad (26)$$

We thus obtain an infinite hierarchy of flow equations for the 2PI vertices (Fig. 1). In all Feynman diagrams shown in this paper, a pair of neighboring external legs corresponds to a bosonic index $\gamma_i = \{\alpha_i, \beta_i\}$. We shall always represent the 2PI two-particle vertex $\bar{\Phi}_{\gamma_1 \gamma_2}^{(2)}$ with the two external legs $\gamma_1 = \{\alpha_1, \beta_1\}$ ($\gamma_2 = \{\alpha_2, \beta_2\}$) on the left (right) hand side of the vertex: $\bar{\Phi}_{\gamma_1 \gamma_2}^{(2)}$ is 2PI as seen from left to right.

Eqs. (25,26) should be supplemented with the initial values of the thermodynamic potential and the 2PI vertices at $\Lambda = \Lambda_0$. Since the cutoff function $\Theta_{\mathbf{k}}$ is chosen such that $C|_{\Lambda_0} = 0$, we easily deduce from the diagrammatic expansion of the LW functional that $\bar{\Sigma}|_{\Lambda_0} = 0$ (i.e. $\bar{G}|_{\Lambda_0} = 0$), $\bar{\Phi}^{(2)}|_{\Lambda_0} = V$, and $\bar{\Phi}^{(n)}|_{\Lambda_0} = 0$ for $n \geq 3$. Using Eq. (11), we also obtain $\Omega|_{\Lambda_0} = \Omega_0|_{\Lambda_0}$ where $\Omega_0 = (2\beta)^{-1} \text{Tr} \ln C$ is the non-interacting thermodynamic potential obtained from the action S_0 . To avoid computing Ω_0 , we shall always calculate $\Delta\Omega = \Omega - \Omega_0$.

For practical calculations, one has to truncate the hierarchy of flow equations (26) by retaining a finite number of low-order vertices. The simplest non-trivial truncation is discussed in the next section. Unless mentioned otherwise, we now drop the ‘‘bar’’ above Green functions and vertices since we shall only consider the case $J = 0$.

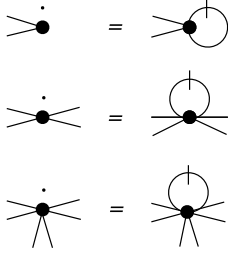


FIG. 1: Diagrammatic representation of the hierarchy (26) of flow equations satisfied by the 2PI vertices $\bar{\Phi}_{\gamma_1 \dots \gamma_n}^{(n)}$. Derivation with respect to l are indicated by dots (vertices) and slashed lines (propagators). A pair of neighboring external legs corresponds to $\gamma_i = \{\alpha_i, \beta_i\}$.

C. One-loop RG equations

1. Flow equations for the 2PI vertices

One-loop RG equations are obtained by neglecting $\Phi^{(n)}$ for $n \geq 4$. This reduces the hierarchy of equations (26) to

$$\begin{aligned} \dot{\Sigma}_{\gamma_1} &= \frac{1}{2} \sum_{\gamma_2} \Phi_{\gamma_1 \gamma_2}^{(2)} \dot{G}_{\gamma_2}, \\ \dot{\Phi}_{\gamma_1 \gamma_2}^{(2)} &= \frac{1}{2} \sum_{\gamma_3} \Phi_{\gamma_1 \gamma_2 \gamma_3}^{(3)} \dot{G}_{\gamma_3}. \end{aligned} \quad (27)$$

In order to close this system of equations, we need an approximate expression of $\Phi^{(3)}$ in terms of $\Phi^{(2)}$ and Σ . Let us start with the second-order contribution to the LW functional,

$$\Phi[G] = -\frac{1}{48} \sum_{\gamma_1, \gamma_2, \gamma_3, \gamma_4} V_{\alpha_1 \beta_3 \alpha_4 \beta_2} V_{\alpha_3 \beta_1 \alpha_2 \beta_4} G_{\gamma_1} G_{\gamma_2} G_{\gamma_3} G_{\gamma_4}. \quad (28)$$

By taking the third-order functional derivative with respect to G , we obtain

$$\begin{aligned} \Phi_{\gamma_1 \gamma_2 \gamma_3}^{(3)} &= -\frac{1}{2} \sum_{\gamma_4} G_{\gamma_4} [V_{\alpha_1 \alpha_3 \alpha_2 \alpha_4} V_{\beta_1 \beta_3 \beta_2 \beta_4} \\ &\quad - V_{\alpha_1 \alpha_3 \beta_2 \alpha_4} V_{\beta_1 \beta_3 \alpha_2 \beta_4} + V_{\alpha_1 \beta_4 \beta_2 \alpha_3} V_{\beta_1 \alpha_4 \alpha_2 \beta_3} \\ &\quad - V_{\alpha_1 \beta_4 \alpha_2 \alpha_3} V_{\beta_1 \alpha_4 \beta_2 \beta_3} - (\alpha_3 \leftrightarrow \beta_3)]. \end{aligned} \quad (29)$$

Replacing V by $\Phi^{(2)}$ in Eq. (29),¹¹ we obtain the one-loop approximation of $\Phi^{(3)}$,

$$\begin{aligned} \Phi_{\gamma_1 \gamma_2 \gamma_3}^{(3)} \Big|_{1\text{loop}} &= -\frac{1}{2} \sum_{\gamma_4} G_{\gamma_4} [\Phi_{\alpha_1 \alpha_3 \alpha_2 \alpha_4}^{(2)} \Phi_{\beta_1 \beta_3 \beta_2 \beta_4}^{(2)} \\ &\quad - \Phi_{\alpha_1 \alpha_3 \beta_2 \alpha_4}^{(2)} \Phi_{\beta_1 \beta_3 \alpha_2 \beta_4}^{(2)} + \Phi_{\alpha_1 \beta_4 \beta_2 \alpha_3}^{(2)} \Phi_{\beta_1 \alpha_4 \alpha_2 \beta_3}^{(2)} \\ &\quad - \Phi_{\alpha_1 \beta_4 \alpha_2 \alpha_3}^{(2)} \Phi_{\beta_1 \alpha_4 \beta_2 \beta_3}^{(2)} - (\alpha_3 \leftrightarrow \beta_3)]. \end{aligned} \quad (30)$$

By working out the symmetry factors of various diagrammatic contributions to $\Phi^{(2)}$ and $\Phi^{(3)}$, one can convince

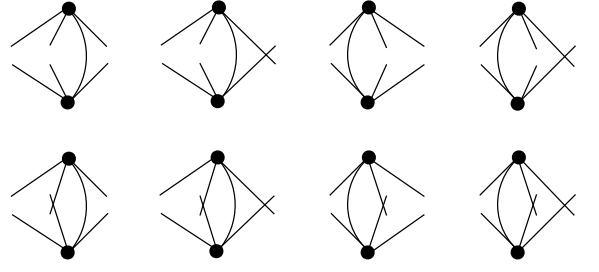


FIG. 2: Diagrammatic representation of $\Phi^{(3)}$ as a function of $\Phi^{(2)}$ within the one-loop approximation. $\Phi^{(2)}$, shown as a black dot, is 2PI as seen from left to right. Signs and symmetry factors are not indicated.

oneself that the overall factor $-1/2$ in Eq. (29) remains unchanged when V is replaced by $\Phi^{(2)}$. $\Phi^{(3)}|_{1\text{loop}}$ is shown diagrammatically in Fig. 2.

Diagrams contributing to $\Phi[G]$, Σ , $\Phi^{(2)}$ and $\Phi^{(3)}$ up to third order in the bare interaction amplitude V are shown in Fig. 3. The $\mathcal{O}(V^2)$ contribution to $\Phi^{(3)}$ is included in the one-loop approximation, but among the three diagrammatic contributions to order V^3 only the first one is retained. The other two are not of the form (30); the second one involves a two-particle-reducible two-particle vertex, while the third one is clearly not of the required type. Thus, a given diagram contributing to the LW functional will generate diagrams for $\Phi^{(3)}$ which may or may not be included in the one-loop approximation. The latter is therefore not a Φ -derivable approximation as it is not based on a truncation of the LW functional. A detailed study of conservation laws and Ward identities in the 2PI RG scheme is beyond the scope of this work and remains to be done.

It should also be noticed that the one-loop approximation, like any approximation of the 2PI vertex $\Phi^{(2)}$, leads to a violation of the crossing symmetries of the two-particle Green function $W^{(2)}$ (e.g. $W_{\alpha_1 \beta_1 \alpha_2 \beta_2}^{(2)} \neq -W_{\alpha_1 \alpha_2 \beta_1 \beta_2}^{(2)}$) and the 1PI two-particle vertex.

From Eqs. (27,30), we finally obtain the one-loop RG equations

$$\begin{aligned} \dot{\Sigma}_{\gamma_1} &= \frac{1}{2} \sum_{\gamma_2} \Phi_{\gamma_1 \gamma_2}^{(2)} \dot{G}_{\gamma_2}, \\ \dot{\Phi}_{\gamma_1 \gamma_2}^{(2)} &= \frac{1}{2} \sum_{\gamma_3, \gamma_4} (\dot{G}_{\gamma_3} G_{\gamma_4} + G_{\gamma_3} \dot{G}_{\gamma_4}) \\ &\quad \times [\Phi_{\alpha_1 \alpha_3 \alpha_4 \beta_2}^{(2)} \Phi_{\beta_1 \beta_3 \beta_4 \alpha_2}^{(2)} - \Phi_{\alpha_1 \alpha_3 \alpha_4 \alpha_2}^{(2)} \Phi_{\beta_1 \beta_3 \beta_4 \beta_2}^{(2)}]. \end{aligned} \quad (31)$$

Eqs. (31) are shown diagrammatically in Fig. 4. There are two differences with respect to the one-loop RG equations obtained within the 1PI RG scheme:^{23,25} (i) the flow equation for the self-energy involves the 2PI two-particle vertex and the derivative \dot{G} of the Green function instead of the 1PI vertex and the ‘‘single-scale propagator’’ $S = -G\dot{C}^{-1}G$; (ii) the one-loop contribution which

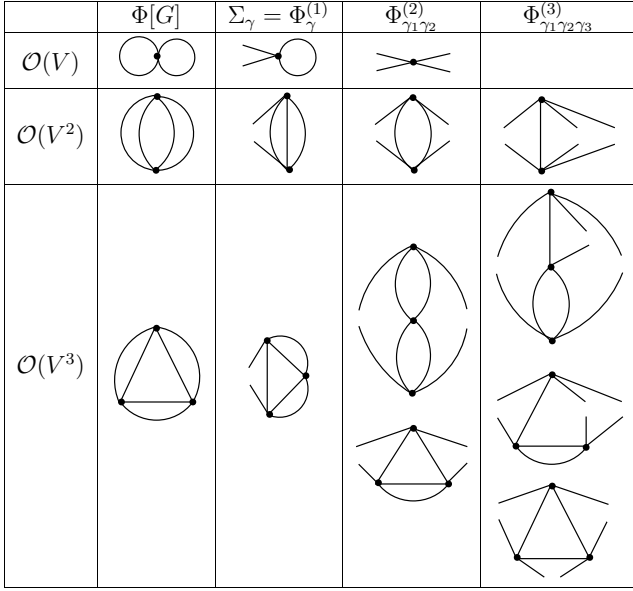


FIG. 3: Diagrams contributing to $\Phi[G]$, Σ_γ , $\Phi_{\gamma_1\gamma_2}^{(2)}$ and $\Phi_{\gamma_1\gamma_2\gamma_3}^{(3)}$ up to third order in the bare interaction vertex V (shown as a (small) black dot). Diagrams obtained by exchanging external legs ($\alpha_i \leftrightarrow \beta_i$) are not shown.

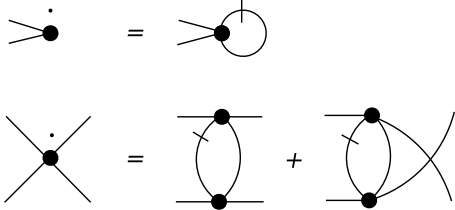


FIG. 4: One-loop flow equations for Σ_γ and $\Phi_{\gamma_1\gamma_2}^{(2)}$. Here and in the following figures, diagrams obtained by exchanging the slashed and non-slashed lines in the one-loop diagrams contributing to $\Phi^{(2)}$ are not shown.

would give a two-particle-reducible contribution to $\Phi^{(2)}$ is absent.

The procedure we have followed to obtain the one-loop RG equation is not unique. Owing to the anti-symmetry of V , one could write $-V_{\alpha_1\beta_3\alpha_4\beta_2}V_{\alpha_3\beta_4\alpha_2\beta_1}$ or $V_{\alpha_4\beta_3\alpha_1\beta_2}V_{\alpha_3\beta_4\alpha_2\beta_1}$ instead of $V_{\alpha_1\beta_3\alpha_4\beta_2}V_{\alpha_3\beta_1\alpha_2\beta_4}$ in Eq. (28). This explains while the one-loop RG equation obtained in Ref. 11,

$$\dot{\Phi}_{\gamma_1\gamma_2}^{(2)} = \sum_{\gamma_3,\gamma_4} \dot{G}_{\gamma_3} G_{\gamma_4} [\Phi_{\alpha_4\alpha_3\alpha_1\beta_2}^{(2)} \Phi_{\beta_4\beta_3\beta_1\alpha_2}^{(2)} - \Phi_{\alpha_4\alpha_3\alpha_1\alpha_2}^{(2)} \Phi_{\beta_4\beta_3\beta_1\beta_2}^{(2)}], \quad (32)$$

differs from ours. This equation can be represented diagrammatic as in Fig. 4, but with the vertices $\Phi^{(2)}$ in the one-loop corrections being 2PI as seen from top to bottom. Eqs. (31,32) lead to different diagram resummations. While the two $\mathcal{O}(V^3)$ contributions to $\Phi^{(2)}$ in Fig. 3 are generated by the equations (31), the first one

is not if one uses Eq. (32). More generally, similar diagrams with an arbitrary number of loops are not included in Eq. (32). These diagrams play a crucial role in most applications of the RG approach to interacting fermion systems. For instance, they describe the exchange of spin fluctuations in a conductor with short-range antiferromagnetic order and may lead to d -wave or other types of unconventional superconductivity. For this reason, we do not expect the one-loop approximation based on Eq. (32) to give reliable results.

2. Relation to the 1PI RG scheme

In this section we show how, starting from Eqs. (31), we can reproduce the one-loop RG equations for the 1PI two-particle vertex $\gamma^{(4)}$ obtained within the 1PI RG scheme. $\gamma^{(4)}$ is defined by

$$G_{c,\gamma_1\gamma_2}^{(4)} = - \sum_{\gamma_3,\gamma_4} G_{\alpha_1\alpha_3} G_{\beta_1\beta_3} G_{\alpha_2\alpha_4} G_{\beta_2\beta_4} \gamma_{\gamma_3\gamma_4}^{(4)}, \quad (33)$$

where

$$\begin{aligned} G_{c,\gamma_1\gamma_2}^{(4)} &= \langle \psi_{\alpha_1} \psi_{\beta_1} \psi_{\alpha_2} \psi_{\beta_2} \rangle - G_{\alpha_1\beta_1} G_{\alpha_2\beta_2} \\ &\quad + G_{\alpha_1\alpha_2} G_{\beta_1\beta_2} - G_{\alpha_1\beta_2} G_{\beta_1\alpha_2} \\ &= W_{\gamma_1\gamma_2}^{(2)} - G_{\alpha_1\beta_2} G_{\beta_1\alpha_2} + G_{\alpha_1\alpha_2} G_{\beta_1\beta_2} \end{aligned} \quad (34)$$

is the (fully) connected two-particle Green function. The Bethe-Salpeter equation (17) implies that $G_c^{(4)}$ satisfies

$$\begin{aligned} \frac{1}{2} \sum_{\gamma_4} [I_{\gamma_1\gamma_4} + \frac{1}{2} \sum_{\gamma_3} \Pi_{\gamma_1\gamma_3} \Phi_{\gamma_3\gamma_4}^{(2)}] G_{c,\gamma_4\gamma_2}^{(4)} = \\ - \frac{1}{4} \sum_{\gamma_3,\gamma_4} \Pi_{\gamma_1\gamma_3} \Phi_{\gamma_3\gamma_4}^{(2)} \Pi_{\gamma_4\gamma_2}, \end{aligned} \quad (35)$$

where

$$\Pi_{\gamma_1\gamma_2} = G_{\alpha_1\beta_2} G_{\beta_1\alpha_2} - G_{\alpha_1\alpha_2} G_{\beta_1\beta_2}. \quad (36)$$

In matrix form, Eqs. (33,35) read

$$\begin{aligned} G_c^{(4)} &= -\Pi\gamma^{(4)}\Pi, \\ (I + \Pi\Phi^{(2)})G_c^{(4)} &= -\Pi\Phi^{(2)}\Pi. \end{aligned} \quad (37)$$

We therefore obtain

$$\begin{aligned} \gamma^{(4)} &= \Phi^{(2)}(I + \Pi\Phi^{(2)})^{-1}, \\ \Phi^{(2)} &= \gamma^{(4)}(I - \Pi\gamma^{(4)})^{-1}. \end{aligned} \quad (38)$$

From these two equations, we deduce the following flow equation for the 1PI vertex $\gamma^{(4)}$,

$$\begin{aligned} \dot{\gamma}^{(4)} &= -\gamma^{(4)}\dot{\Pi}\gamma^{(4)} + \gamma^{(4)}(\Phi^{(2)})^{-1}\dot{\Phi}^{(2)}(\Phi^{(2)})^{-1}\gamma^{(4)} \\ &= -\gamma^{(4)}\dot{\Pi}\gamma^{(4)} + (I - \gamma^{(4)}\Pi)\dot{\Phi}^{(2)}(I - \Pi\gamma^{(4)}). \end{aligned} \quad (39)$$

We can now reproduce the one-loop RG equations derived within the 1PI RG scheme by expanding the rhs

of Eq. (39) to second order in $\gamma^{(4)}$. Since $\Phi^{(2)} = \gamma^{(4)} + \mathcal{O}[(\gamma^{(4)})^2]$ and $\dot{\Phi}^{(2)} = \mathcal{O}[(\Phi^{(2)})^2]$, Eq. (39) gives $\dot{\gamma}^{(4)} = -\gamma^{(4)}\dot{\Pi}\gamma^{(4)} + \dot{\Phi}^{(2)}$ where, to order $(\gamma^{(4)})^2$, $\dot{\Phi}^{(2)}$ is given by Eq. (31) with $\Phi^{(2)}$ replaced by $\gamma^{(4)}$ in the rhs. This eventually gives

$$\begin{aligned} \dot{\gamma}_{\gamma_1\gamma_2}^{(4)} = & -\frac{1}{2} \sum_{\gamma_3, \gamma_4} (\dot{G}_{\alpha_3\beta_4} G_{\beta_3\alpha_4} + G_{\alpha_3\beta_4} \dot{G}_{\beta_3\alpha_4}) \\ & \times [\gamma_{\alpha_1\beta_1\alpha_3\beta_3}^{(4)} \gamma_{\alpha_4\beta_4\alpha_2\beta_2}^{(4)} - \gamma_{\alpha_1\alpha_3\beta_3\beta_2}^{(4)} \gamma_{\beta_1\beta_4\alpha_4\alpha_2}^{(4)} \\ & + \gamma_{\alpha_1\alpha_3\beta_3\alpha_2}^{(4)} \gamma_{\beta_1\beta_4\alpha_4\beta_2}^{(4)}]. \end{aligned} \quad (40)$$

To lowest order in $\gamma^{(4)}$, the flow equation (31) for the self-energy becomes

$$\dot{\Sigma}_{\gamma_1} = \frac{1}{2} \sum_{\gamma_2} \gamma_{\gamma_1\gamma_2}^{(4)} \dot{G}_{\gamma_2}. \quad (41)$$

Eqs. (40,41) agrees with the equations derived within the 1PI RG scheme^{23,25} with the ‘‘single-scale propagator’’ $S = -G\dot{C}^{-1}G$ replaced by \dot{G} .

D. One-loop RG equations in the normal phase

In this section, we consider the one-loop RG equations in the absence of broken symmetry. We denote the position, time and spin indices by X so that $\alpha = (X, c)$, $\psi(X+) = \psi^*(X)$, $\psi(X-) = \psi(X)$, and $\int dX = \int_0^\beta d\tau \int d^d r \sum_\sigma$. The single-particle Green function is then given by

$$G(X_1-, X_2+) = \langle \psi(X_1)\psi^*(X_2) \rangle \equiv G(X_1, X_2), \quad (42)$$

with $G(X_1+, X_2-) = -G(X_2, X_1)$. $G(X_1c, X_2c)$ vanishes in the normal phase. G satisfies the Dyson equation

$$\begin{aligned} G(X_1, X_2) = & C(X_1, X_2) \\ & - \int dX_3 dX_4 C(X_1, X_3) \Sigma(X_3, X_4) G(X_4, X_2) \end{aligned} \quad (43)$$

with

$$\Sigma(X_1, X_2) = \Sigma(X_1+, X_2-) \quad (44)$$

the self-energy. In the normal phase, the 2PI two-particle vertex $\Phi^{(2)}(X_1c_1, X_2c_2, X_3c_3, X_4c_4)$ vanishes if $\sum_i c_i \neq 0$. Distinguishing between the particle-particle (pp) and particle-hole (ph) channels, we introduce

$$\begin{aligned} \Phi_{\text{pp}}^{(2)}(X_1, X_2, X_3, X_4) &= \Phi^{(2)}(X_1+, X_2+, X_3-, X_4-), \\ \Phi_{\text{ph}}^{(2)}(X_1, X_2, X_3, X_4) &= \Phi^{(2)}(X_1+, X_2-, X_3+, X_4-). \end{aligned} \quad (45)$$

Note that in Eqs. (45), we have singled out one of the two ph channels. The 2PI vertex in the other ph channel is related to $\Phi_{\text{ph}}^{(2)}$ by

$$\Phi^{(2)}(X_1+, X_2-, X_3-, X_4+) = -\Phi_{\text{ph}}^{(2)}(X_1, X_2, X_4, X_3). \quad (46)$$

Since the one-loop approximation conserves the crossing symmetry $\Phi_{\gamma_1\{\alpha_2\beta_2\}}^{(2)} = -\Phi_{\gamma_1\{\beta_2\alpha_2\}}^{(2)}$ (as obvious from Fig. 4), it is possible to consider a single ph channel. The symmetry properties of $\Phi_{\gamma_1\gamma_2}^{(2)}$ [Eqs. (15)] imply

$$\begin{aligned} \Phi_{\text{pp}}^{(2)}(X_1, X_2, X_3, X_4) &= -\Phi_{\text{pp}}^{(2)}(X_2, X_1, X_3, X_4) \\ &= -\Phi_{\text{pp}}^{(2)}(X_1, X_2, X_4, X_3), \\ \Phi_{\text{ph}}^{(2)}(X_1, X_2, X_3, X_4) &= \Phi_{\text{ph}}^{(2)}(X_3, X_4, X_1, X_2). \end{aligned} \quad (47)$$

The RG equation for the self-energy can be written as

$$\begin{aligned} \dot{\Sigma}(X_1, X_2) &= \frac{1}{2} \sum_{c=\pm} \int dX_3 dX_4 \dot{G}(X_3c, X_4\bar{c}) \\ &\quad \times \Phi^{(2)}(X_1+, X_2-, X_3c, X_4\bar{c}) \\ &= - \int dX_3 dX_4 \dot{G}(X_4, X_3) \\ &\quad \times \Phi_{\text{ph}}^{(2)}(X_1, X_2, X_3, X_4), \end{aligned} \quad (48)$$

where $\bar{c} = -c$. A similar calculation for the two-particle vertices $\Phi_{\text{pp}}^{(2)}$ and $\Phi_{\text{ph}}^{(2)}$ yields

$$\begin{aligned} \dot{\Phi}_{\text{pp}}^{(2)}(X_i) &= -\frac{1}{2} \int dX'_1 dX'_2 dX'_3 dX'_4 [G(X'_2, X'_1) \dot{G}(X'_3, X'_4) + (G \leftrightarrow \dot{G})] [\Phi_{\text{pp}}^{(2)}(X_1, X'_1, X'_3, X_4) \Phi_{\text{ph}}^{(2)}(X_2, X'_2, X'_4, X_3) \\ &\quad + \Phi_{\text{ph}}^{(2)}(X_1, X'_2, X'_4, X_4) \Phi_{\text{pp}}^{(2)}(X_2, X'_1, X'_3, X_3) - (X_3 \leftrightarrow X_4)], \\ \dot{\Phi}_{\text{ph}}^{(2)}(X_i) &= -\frac{1}{2} \int dX'_1 dX'_2 dX'_3 dX'_4 [G(X'_2, X'_1) \dot{G}(X'_3, X'_4) + (G \leftrightarrow \dot{G})] [\Phi_{\text{pp}}^{(2)}(X_1, X'_1, X'_3, X_4) \Phi_{\text{pp}}^{(2)}(X'_4, X_3, X_2, X'_2) \\ &\quad + \Phi_{\text{ph}}^{(2)}(X_1, X'_2, X'_4, X_4) \Phi_{\text{ph}}^{(2)}(X'_1, X_2, X_3, X'_3) + \Phi_{\text{ph}}^{(2)}(X_1, X'_2, X_3, X'_3) \Phi_{\text{ph}}^{(2)}(X'_1, X_2, X'_4, X_4)], \end{aligned} \quad (49)$$

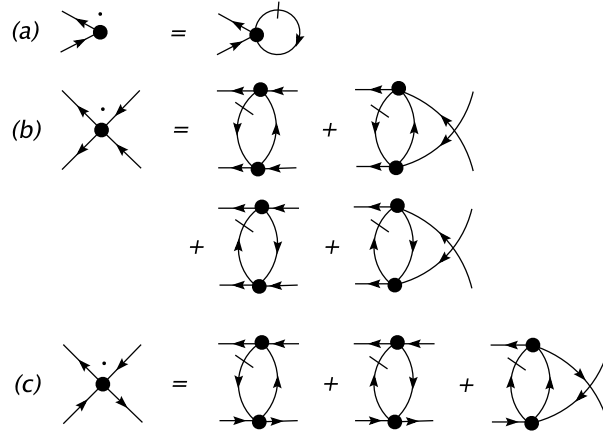


FIG. 5: One-loop RG equations for Σ (a), $\Phi_{\text{pp}}^{(2)}$ (b) and $\Phi_{\text{ph}}^{(2)}$ (c) in the normal phase.

where we use the short-hand notation $\Phi^{(2)}(X_i) = \Phi^{(2)}(X_1, X_2, X_3, X_4)$. Eqs. (49) are shown diagrammatically in Fig. 5.

In spin-rotation invariant systems, it is convenient to write $\Phi_{\text{pp}}^{(2)}$ and $\Phi_{\text{ph}}^{(2)}$ in the triplet/singlet and charge/spin basis, respectively,

$$\begin{aligned}\Phi_{\text{pp},\sigma_i}^{(2)}(x_i) &= \Phi_{\text{t}}^{(2)}(x_i)I_{\sigma_3\sigma_4}^{\sigma_1\sigma_2} + \Phi_{\text{s}}^{(2)}(x_i)T_{\sigma_3\sigma_4}^{\sigma_1\sigma_2}, \\ \Phi_{\text{ph},\sigma_i}^{(2)}(x_i) &= \Phi_{\text{ch}}^{(2)}(x_i)\delta_{\sigma_1,\sigma_2}\delta_{\sigma_3,\sigma_4} + \Phi_{\text{sp}}^{(2)}(x_i)\boldsymbol{\sigma}_{\sigma_1,\sigma_2} \cdot \boldsymbol{\sigma}_{\sigma_3,\sigma_4},\end{aligned}\quad (50)$$

($X = (x, \sigma)$, $x = (\mathbf{r}, \tau)$), where

$$I_{\sigma_3\sigma_4}^{\sigma_1\sigma_2} = \frac{1}{2}(\delta_{\sigma_1,\sigma_4}\delta_{\sigma_2,\sigma_3} + \delta_{\sigma_1,\sigma_3}\delta_{\sigma_2,\sigma_4}), \quad T_{\sigma_3\sigma_4}^{\sigma_1\sigma_2} = \frac{1}{2}(\delta_{\sigma_1,\sigma_4}\delta_{\sigma_2,\sigma_3} - \delta_{\sigma_1,\sigma_3}\delta_{\sigma_2,\sigma_4}), \quad (51)$$

and $\boldsymbol{\sigma} = (\sigma^x, \sigma^y, \sigma^z)$ stands for the Pauli matrices. From Eqs. (47), we deduce the following symmetry properties

$$\begin{aligned}\Phi_{\text{t}}^{(2)}(x_1, x_2, x_3, x_4) &= -\Phi_{\text{t}}^{(2)}(x_2, x_1, x_3, x_4) = -\Phi_{\text{t}}^{(2)}(x_1, x_2, x_4, x_3), \\ \Phi_{\text{s}}^{(2)}(x_1, x_2, x_3, x_4) &= \Phi_{\text{s}}^{(2)}(x_2, x_1, x_3, x_4) = \Phi_{\text{s}}^{(2)}(x_1, x_2, x_4, x_3), \\ \Phi_{\text{ch,sp}}^{(2)}(x_1, x_2, x_3, x_4) &= \Phi_{\text{ch,sp}}^{(2)}(x_3, x_4, x_1, x_2).\end{aligned}\quad (52)$$

Performing the sum over spin indices in Eqs. (48,49), we obtain the flow equations satisfied by Σ , $\Phi_{\text{t,s}}^{(2)}$ and $\Phi_{\text{ch,sp}}^{(2)}$,

$$\dot{\Sigma}(x_1, x_2) = -2 \int dx_3 dx_4 \dot{G}(x_4, x_3) \Phi_{\text{ch}}^{(2)}(x_1, x_2, x_3, x_4), \quad (53)$$

$$\begin{aligned}
\dot{\Phi}_t^{(2)}(x_i) &= -\frac{1}{2} \int dx'_1 dx'_2 dx'_3 dx'_4 B(x'_2, x'_1, x'_3, x'_4) \\
&\quad \times \left[\left(\Phi_t^{(2)}(x_1, x'_1, x'_3, x_4) \Phi_{\text{ch}}^{(2)}(x_2, x'_2, x'_4, x_3) + 2\Phi_t^{(2)} \Phi_{\text{sp}}^{(2)} + \Phi_s^{(2)} \Phi_{\text{sp}}^{(2)} \right) \right. \\
&\quad \left. + \left(\Phi_{\text{ch}}^{(2)}(x_1, x'_2, x'_4, x_4) \Phi_t^{(2)}(x_2, x'_1, x'_3, x_3) + 2\Phi_{\text{sp}}^{(2)} \Phi_t^{(2)} + \Phi_{\text{sp}}^{(2)} \Phi_s^{(2)} \right) - (x_3 \leftrightarrow x_4) \right], \\
\dot{\Phi}_s^{(2)}(x_i) &= -\frac{1}{2} \int dx'_1 dx'_2 dx'_3 dx'_4 B(x'_2, x'_1, x'_3, x'_4) \\
&\quad \times \left[\left(\Phi_s^{(2)}(x_1, x'_1, x'_3, x_4) \Phi_{\text{ch}}^{(2)}(x_2, x'_2, x'_4, x_3) + 3\Phi_t^{(2)} \Phi_{\text{sp}}^{(2)} \right) \right. \\
&\quad \left. + \Phi_{\text{ch}}^{(2)}(x_1, x'_2, x'_4, x_4) \Phi_s^{(2)}(x_2, x'_1, x'_3, x_3) + 3\Phi_{\text{sp}}^{(2)} \Phi_t^{(2)} \right] + (x_3 \leftrightarrow x_4), \\
\dot{\Phi}_{\text{ch}}^{(2)}(x_i) &= -\frac{1}{2} \int dx'_1 dx'_2 dx'_3 dx'_4 B(x'_2, x'_1, x'_3, x'_4) \\
&\quad \times \left[\left(\frac{3}{4} \Phi_t^{(2)}(x_1, x'_1, x'_3, x_4) \Phi_t^{(2)}(x'_4, x_3, x_2, x'_2) + \frac{1}{4} \Phi_s^{(2)} \Phi_s^{(2)} \right) \right. \\
&\quad \left. + \left(\Phi_{\text{ch}}^{(2)}(x_1, x'_2, x'_4, x_4) \Phi_{\text{ch}}^{(2)}(x'_1, x_2, x_3, x'_3) + 3\Phi_{\text{sp}}^{(2)} \Phi_{\text{sp}}^{(2)} \right) \right. \\
&\quad \left. + \left(\Phi_{\text{ch}}^{(2)}(x_1, x'_2, x_3, x'_3) \Phi_{\text{ch}}^{(2)}(x'_1, x_2, x'_4, x_4) + 3\Phi_{\text{sp}}^{(2)} \Phi_{\text{sp}}^{(2)} \right) \right], \\
\dot{\Phi}_{\text{sp}}^{(2)}(x_i) &= -\frac{1}{2} \int dx'_1 dx'_2 dx'_3 dx'_4 B(x'_2, x'_1, x'_3, x'_4) \\
&\quad \times \left[\left(\frac{1}{2} \Phi_t^{(2)}(x_1, x'_1, x'_3, x_4) \Phi_t^{(2)}(x'_4, x_3, x_2, x'_2) + \frac{1}{4} \Phi_t^{(2)} \Phi_s^{(2)} + \frac{1}{4} \Phi_s^{(2)} \Phi_t^{(2)} \right) \right. \\
&\quad \left. + \left(\Phi_{\text{ch}}^{(2)}(x_1, x'_2, x'_4, x_4) \Phi_{\text{sp}}^{(2)}(x'_1, x_2, x_3, x'_3) + \Phi_{\text{sp}}^{(2)} \Phi_{\text{ch}}^{(2)} + 2\Phi_{\text{sp}}^{(2)} \Phi_{\text{sp}}^{(2)} \right) \right. \\
&\quad \left. + \left(\Phi_{\text{ch}}^{(2)}(x_1, x'_2, x_3, x'_3) \Phi_{\text{sp}}^{(2)}(x'_1, x_2, x'_4, x_4) + \Phi_{\text{sp}}^{(2)} \Phi_{\text{ch}}^{(2)} - 2\Phi_{\text{sp}}^{(2)} \Phi_{\text{sp}}^{(2)} \right) \right], \tag{54}
\end{aligned}$$

where

$$B(x_1, x_2, x_3, x_4) = G(x_1, x_2) \dot{G}(x_3, x_4) + (G \leftrightarrow \dot{G}). \tag{55}$$

Due to spin-rotation invariance, the single-particle Green function $G_{\sigma_1 \sigma_2}(x_1, x_2) = \delta_{\sigma_1, \sigma_2} G(x_1, x_2)$ and the self-energy $\Sigma_{\sigma_1 \sigma_2}(x_1, x_2) = \delta_{\sigma_1, \sigma_2} \Sigma(x_1, x_2)$. In Eqs. (54), we have grouped inside parenthesis terms with identical dependences on the variables x_i, x'_i and thus avoided unnecessary repetitions of the latter.

E. Response functions in the normal phase

Once we have solved the RG equations (53,54) and determined the self-energy Σ and the 2PI vertex $\Phi^{(2)}$, we can obtain the two-particle Green functions $W^{(2)}$ and the response functions from the Bethe-Salpeter equation (17).

We define triplet- and singlet-pairing fields, and charge- and spin-density fields by

$$\begin{aligned}
O_t^\nu(x_1, x_2) &= \begin{cases} \psi_\uparrow(x_1) \psi_\uparrow(x_2) & \text{if } \nu = 1, \\ \frac{1}{\sqrt{2}} \sum_\sigma \psi_\sigma(x_1) \psi_{\bar{\sigma}}(x_2) & \text{if } \nu = 0, \\ \psi_\downarrow(x_1) \psi_\downarrow(x_2) & \text{if } \nu = -1, \end{cases} \\
O_s(x_1, x_2) &= \frac{1}{\sqrt{2}} \sum_\sigma \sigma \psi_\sigma(x_1) \psi_{\bar{\sigma}}(x_2), \\
\rho(x_1, x_2) &= \sum_\sigma \psi_\sigma^*(x_1) \psi_\sigma(x_2), \\
\mathbf{S}(x_1, x_2) &= \sum_{\sigma_1, \sigma_2} \psi_{\sigma_1}^*(x_1) \boldsymbol{\sigma}_{\sigma_1, \sigma_2} \psi_{\sigma_2}(x_2), \tag{56}
\end{aligned}$$

($\bar{\sigma} = -\sigma$), and the corresponding response functions

$$\begin{aligned}
\chi_t(x_i) &= \langle O_t^\nu(x_1, x_2) O_t^{\nu*}(x_4, x_3) \rangle = \begin{cases} W_{\text{pp}, \uparrow\uparrow\uparrow\uparrow}^{(2)}(x_i) & \text{if } \nu = 1, \\ \frac{1}{2} \sum_{\sigma_1, \sigma_3} W_{\text{pp}, \sigma_1 \bar{\sigma}_1 \sigma_3 \bar{\sigma}_3}^{(2)}(x_i) & \text{if } \nu = 0, \\ W_{\text{pp}, \downarrow\downarrow\downarrow\downarrow}^{(2)}(x_i) & \text{if } \nu = -1, \end{cases} \\
\chi_s(x_i) &= \langle O_s(x_1, x_2) O_s^*(x_4, x_3) \rangle = \frac{1}{2} \sum_{\sigma_1, \sigma_3} \sigma_1 \bar{\sigma}_3 W_{\text{pp}, \sigma_1 \bar{\sigma}_1 \sigma_3 \bar{\sigma}_3}^{(2)}(x_i), \\
\chi_{\text{ch}}(x_i) &= \langle \rho(x_1, x_2) \rho(x_3, x_4) \rangle = \sum_{\sigma_1, \sigma_3} W_{\text{ph}, \sigma_1 \sigma_1 \sigma_3 \sigma_3}^{(2)}(x_2, x_1, x_4, x_3), \\
\chi_{\text{sp}}(x_i) &= \langle S^\nu(x_1, x_2) S^\nu(x_3, x_4) \rangle = \sum_{\sigma_1, \sigma_2, \sigma_3, \sigma_4} \sigma_{\sigma_1, \sigma_2}^\nu \sigma_{\sigma_3, \sigma_4}^\nu W_{\text{ph}, \sigma_2 \sigma_1 \sigma_4 \sigma_3}^{(2)}(x_2, x_1, x_4, x_3), \tag{57}
\end{aligned}$$

where $W_{\text{pp}, \sigma_i}^{(2)}(x_i) = W_{\sigma_i}^{(2)}(x_1-, x_2-, x_3+, x_4+)$ and $W_{\text{ph}, \sigma_i}^{(2)}(x_i) = W_{\sigma_i}^{(2)}(x_1-, x_2+, x_3-, x_4+)$ are the two-particle Green functions in the pp and ph channels, respectively. They satisfy the Bethe-Salpeter equations [see Eq. (17)]

$$\begin{aligned}
W_{\text{pp}, \sigma_i}^{(2)}(x_i) &= \delta_{\sigma_1, \sigma_4} \delta_{\sigma_2, \sigma_3} G(x_1, x_4) G(x_2, x_3) - \delta_{\sigma_1, \sigma_3} \delta_{\sigma_2, \sigma_4} G(x_1, x_3) G(x_2, x_4) \\
&\quad + \frac{1}{2} \sum_{\sigma, \sigma'} \int dx'_1 dx'_2 dx'_3 dx'_4 G(x_1, x'_1) G(x_2, x'_2) \Phi_{\text{pp}, \sigma_1 \sigma_2 \sigma \sigma'}^{(2)}(x'_1, x'_2, x'_3, x'_4) W_{\text{pp}, \sigma \sigma' \sigma_3 \sigma_4}^{(2)}(x'_3, x'_4, x_3, x_4), \\
W_{\text{ph}, \sigma_i}^{(2)}(x_i) &= -\delta_{\sigma_1, \sigma_4} \delta_{\sigma_2, \sigma_3} G(x_1, x_4) G(x_3, x_2) \\
&\quad + \sum_{\sigma, \sigma'} \int dx'_1 dx'_2 dx'_3 dx'_4 G(x_1, x'_1) G(x'_2, x_2) \Phi_{\text{ph}, \sigma_1 \sigma_2 \sigma \sigma'}^{(2)}(x'_1, x'_2, x'_3, x'_4) W_{\text{ph}, \sigma \sigma' \sigma_3 \sigma_4}^{(2)}(x'_4, x'_3, x_3, x_4). \tag{58}
\end{aligned}$$

From Eqs. (58) we deduce

$$\begin{aligned}
\chi_{\mu=t,s}(x_i) &= G(x_1, x_4) G(x_2, x_3) \mp G(x_1, x_3) G(x_2, x_4) \\
&\quad - \frac{1}{2} \int dx'_1 dx'_2 dx'_3 dx'_4 G(x_1, x'_1) G(x_2, x'_2) \Phi_\mu^{(2)}(x'_1, x'_2, x'_3, x'_4) \chi_\mu(x'_4, x'_3, x_3, x_4), \\
\chi_{\mu=\text{ch}, \text{sp}}(x_i) &= -2G(x_4, x_1) G(x_2, x_3) \\
&\quad + 2 \int dx'_1 dx'_2 dx'_3 dx'_4 G(x_2, x'_1) G(x'_2, x_1) \Phi_\mu^{(2)}(x'_1, x'_2, x'_3, x'_4) \chi_\mu(x'_3, x'_4, x_3, x_4). \tag{59}
\end{aligned}$$

Eqs. (59) enable ones to determine the response functions from the knowledge of the single-particle Green function G and the 2PI vertex $\Phi^{(2)}$.

In many cases, useful information can also be drawn from the 1PI two-particle vertex $\gamma^{(4)}$. Rewriting the relation (38) between $\gamma^{(4)}$ and $\Phi^{(2)}$ as

$$\gamma_{\gamma_1 \gamma_2}^{(4)} = \Phi_{\gamma_1 \gamma_2}^{(2)} - \frac{1}{2} \sum_{\gamma_3 \gamma_4} \Phi_{\gamma_1 \gamma_3}^{(2)} G_{\alpha_3 \beta_4} G_{\beta_3 \alpha_4} \gamma_{\gamma_4 \gamma_2}^{(4)}, \tag{60}$$

and considering this equation in the pp and ph channels, we obtain

$$\begin{aligned}
\gamma_{\mu=t,s}^{(4)}(x_i) &= \Phi_\mu^{(2)}(x_i) - \frac{1}{2} \int dx'_1 dx'_2 dx'_3 dx'_4 \\
&\quad \times \Phi_\mu^{(2)}(x_1, x_2, x'_1, x'_2) G(x'_1, x'_3) G(x'_2, x'_4) \\
&\quad \times \gamma_\mu^{(4)}(x'_4, x'_3, x_3, x_4), \\
\gamma_{\mu=\text{ch}, \text{sp}}^{(4)}(x_i) &= \Phi_\mu^{(2)}(x_i) + 2 \int dx'_1 dx'_2 dx'_3 dx'_4 \\
&\quad \times \Phi_\mu^{(2)}(x_1, x_2, x'_1, x'_2) G(x'_3, x'_1) G(x'_2, x'_4) \\
&\quad \times \gamma_\mu^{(4)}(x'_4, x'_3, x_3, x_4). \tag{61}
\end{aligned}$$

F. Ginzburg-Landau expansion

An essential feature of the 2PI scheme is the possibility to continue the RG flow in a broken-symmetry phase. This will be illustrated in the next section in the frame-

work of the BCS theory, and further discussed in the concluding section. As a byproduct, one can also derive the Ginzburg-Landau expansion of the thermodynamical potential in the vicinity of a phase transition. The interest of such an approach is that only the solution of the RG equations with no symmetry breaking is necessary. When several instabilities compete at low temperature, the derivation of the Ginzburg-Landau expansion is expected to be much simpler than the full solution of the RG equations in the broken-symmetry phase.

We introduce the Legendre transform $F[\Sigma]$ of the LW functional $\Phi[G]$,

$$F[\Sigma] = \Phi[G] + \frac{1}{2}\text{Tr}(G\Sigma), \quad (62)$$

where $G \equiv G[\Sigma]$ is a functional of Σ obtained by inverting $\Sigma_\gamma = \delta\Phi[G]/\delta G_\gamma$. Here and in the following, we assume vanishing external sources ($J = 0$), and denote \bar{G} , $\bar{\Sigma}$ by G , Σ , etc. $F[\Sigma]$ satisfies

$$\frac{\delta F[\Sigma]}{\delta \Sigma_\gamma} = -G_\gamma. \quad (63)$$

The functional $F[\Sigma]$ allows us to rewrite $\Gamma[G]$ as a functional of the self-energy,⁵³

$$\begin{aligned} \Gamma[\Sigma] &= -\frac{1}{2}\text{Tr}\ln(C^{-1} + \Sigma) + \frac{1}{2}\text{Tr}(G\Sigma) + \Phi[G] \\ &= -\frac{1}{2}\text{Tr}\ln(C^{-1} + \Sigma) + F[\Sigma], \end{aligned} \quad (64)$$

which is stationary at the equilibrium self-energy $\Sigma \equiv \bar{\Sigma}$,

$$\frac{\delta \Gamma[\Sigma]}{\delta \Sigma_\gamma} = 0. \quad (65)$$

We now write the self-energy $\Sigma = \Sigma_N + \Delta$ as the sum of a normal part Σ_N and an anomalous part Δ which violates some symmetries of the normal phase. Δ is an order parameter for the phase transition. It can include different kinds of symmetry breaking, such as antiferromagnetism and superconductivity. If we are able to solve the flow equations in the normal phase, i.e. fixing $\Delta = 0$, we can consider $\Gamma[\Delta] \equiv \Gamma[\Sigma_N + \Delta]$ as a functional of the (unknown) anomalous self-energy Δ . The latter is then determined from the stationary condition (65),

$$\frac{\delta \Gamma[\Delta]}{\delta \Delta_\gamma} = 0. \quad (66)$$

A crucial point here is that the 2PI flow equations with $\Delta = 0$ can be continued below the actual phase transition temperature T_c , since the 2PI vertices do not become singular at the transition. The functional $\Gamma[\Delta]$ can therefore be determined below T_c , where the stationary value of Δ [Eq. (66)] is finite.

In the vicinity of the phase transition, where Δ is small, we expand $\Gamma[\Delta]$ to fourth order,

$$\begin{aligned} \Gamma[\Delta] &= \Gamma_N + \frac{1}{4}\text{Tr}(G_N\Delta)^2 + \frac{1}{2!}\frac{1}{2^2}\sum_{\gamma_1,\gamma_2} F_{\gamma_1\gamma_2}^{(2)}\Delta_{\gamma_1}\Delta_{\gamma_2} \\ &\quad - \frac{1}{6}\text{Tr}(G_N\Delta)^3 + \frac{1}{3!}\frac{1}{2^3}\sum_{\gamma_1,\gamma_2,\gamma_3} F_{\gamma_1\gamma_2\gamma_3}^{(3)}\Delta_{\gamma_1}\Delta_{\gamma_2}\Delta_{\gamma_3} \\ &\quad + \frac{1}{8}\text{Tr}(G_N\Delta)^4 + \frac{1}{4!}\frac{1}{2^4}\sum_{\gamma_1,\gamma_2,\gamma_3,\gamma_4} F_{\gamma_1\gamma_2\gamma_3\gamma_4}^{(4)} \\ &\quad \times \Delta_{\gamma_1}\Delta_{\gamma_2}\Delta_{\gamma_3}\Delta_{\gamma_4}, \end{aligned} \quad (67)$$

where $\beta^{-1}\Gamma_N = \beta^{-1}\Gamma[\Sigma_N] = \Omega_N$ is the thermodynamic potential and G_N the Green function in the normal phase, and

$$F_{\gamma_1\cdots\gamma_n}^{(n)} = \left. \frac{\delta^{(n)}F[\Sigma]}{\delta \Sigma_{\gamma_1}\cdots\delta \Sigma_{\gamma_n}} \right|_{\Sigma_N}. \quad (68)$$

If, as in most one-loop approximations, one ignores the normal phase self-energy ($G_N = C$), the evaluation of the terms $\text{Tr}(G_N\Delta)^n$ does not raise any difficulty. The determination of $\Gamma[\Delta]$ then requires the calculation of the coefficients $F^{(n)}$. These can be related to the 2PI vertices $\Phi^{(n)}$ by taking functional derivatives of Eq. (63) with respect to G . The first-order derivative gives

$$-\frac{1}{2}\sum_{\gamma_3} \left. \frac{\delta^{(2)}\Phi[G]}{\delta G_{\gamma_1}\delta G_{\gamma_3}} \right|_{G_N} \left. \frac{\delta^{(2)}F[\Sigma]}{\delta \Sigma_{\gamma_3}\delta \Sigma_{\gamma_2}} \right|_{\Sigma_N} = I_{\gamma_1\gamma_2}, \quad (69)$$

i.e.

$$(F^{(2)})_{\gamma_1\gamma_2}^{-1} = -\Phi_{\gamma_1\gamma_2}^{(2)}. \quad (70)$$

Higher-order derivatives yield

$$\begin{aligned} F_{\gamma_1\gamma_2\gamma_3}^{(3)} &= -\frac{1}{8}\sum_{\gamma'_1,\gamma'_2,\gamma'_3} \Phi_{\gamma'_1\gamma'_2\gamma'_3}^{(3)} F_{\gamma'_1\gamma_1}^{(2)} F_{\gamma'_2\gamma_2}^{(2)} F_{\gamma'_3\gamma_3}^{(2)}, \\ F_{\gamma_1\gamma_2\gamma_3\gamma_4}^{(4)} &= \frac{1}{16}\sum_{\gamma'_1,\gamma'_2,\gamma'_3,\gamma'_4} \Phi_{\gamma'_1\gamma'_2\gamma'_3\gamma'_4}^{(4)} F_{\gamma'_1\gamma_1}^{(2)} F_{\gamma'_2\gamma_2}^{(2)} F_{\gamma'_3\gamma_3}^{(2)} F_{\gamma'_4\gamma_4}^{(2)} \\ &\quad - \frac{1}{8}\sum_{\gamma'_1,\gamma'_2,\gamma'_3} \Phi_{\gamma'_1\gamma'_2\gamma'_3}^{(3)} [F_{\gamma_4\gamma'_1\gamma_1}^{(3)} F_{\gamma'_2\gamma_2}^{(2)} F_{\gamma'_3\gamma_3}^{(2)} \\ &\quad + F_{\gamma'_1\gamma_1}^{(2)} F_{\gamma_4\gamma'_2\gamma_2}^{(3)} F_{\gamma'_3\gamma_3}^{(2)} + F_{\gamma'_1\gamma_1}^{(2)} F_{\gamma'_2\gamma_2}^{(2)} F_{\gamma_4\gamma'_3\gamma_3}^{(3)}]. \end{aligned} \quad (71)$$

These equations simplify within the one-loop approximation, since $\Phi^{(n)}$ vanishes for $n \geq 4$ and $\Phi^{(3)}$ can be expressed in terms of $\Phi^{(2)}$. $F^{(3)}$ and $F^{(4)}$ are then essentially determined by $\Phi^{(2)}$ and $F^{(2)}$. Writing the equation $\Phi^{(2)}F^{(2)} = -I$ in the pp and ph channels, we obtain

$$\begin{aligned} &\frac{1}{2}\int dXdX'\Phi_{\text{pp}}^{(2)}(X_1, X_2, X, X')F_{\text{pp}}^{(2)}(X', X, X_3, X_4) = \\ &-\delta(X_1 - X_4)\delta(X_2 - X_3) + \delta(X_1 - X_3)\delta(X_2 - X_4), \\ &\int dXdX'\Phi_{\text{ph}}^{(2)}(X_1, X_2, X, X')F_{\text{ph}}^{(2)}(X', X, X_3, X_4) = \\ &-\delta(X_1 - X_4)\delta(X_2 - X_3), \end{aligned} \quad (72)$$

where

$$\begin{aligned} F_{\text{pp}}^{(2)}(X_1, X_2, X_3, X_4) &= F^{(2)}(X_1-, X_2-, X_3+, X_4+), \\ F_{\text{ph}}^{(2)}(X_1, X_2, X_3, X_4) &= F^{(2)}(X_1-, X_2+, X_3-, X_4+). \end{aligned} \quad (73)$$

For a spin-rotation invariant system, we finally deduce

$$\begin{aligned} &\int dx dx' \Phi_{\text{t}}^{(2)}(x_1, x_2, x, x') F_{\text{t}}^{(2)}(x', x, x_3, x_4) = \\ &- 2[\delta(x_1 - x_4)\delta(x_2 - x_3) - \delta(x_1 - x_3)\delta(x_2 - x_4)], \\ &\int dx dx' \Phi_{\text{s}}^{(2)}(x_1, x_2, x, x') F_{\text{s}}^{(2)}(x', x, x_3, x_4) = \\ &- 2[\delta(x_1 - x_4)\delta(x_2 - x_3) + \delta(x_1 - x_3)\delta(x_2 - x_4)], \\ &\int dx dx' \Phi_{\text{ch}}^{(2)}(x_1, x_2, x, x') F_{\text{ch}}^{(2)}(x', x, x_3, x_4) = \\ &\quad - \frac{1}{4}\delta(x_1 - x_4)\delta(x_2 - x_3), \\ &\int dx dx' \Phi_{\text{sp}}^{(2)}(x_1, x_2, x, x') F_{\text{sp}}^{(2)}(x', x, x_3, x_4) = \\ &\quad - \frac{1}{4}\delta(x_1 - x_4)\delta(x_2 - x_3). \end{aligned} \quad (74)$$

where $F_{\text{t,s}}^{(2)}$ are the triplet and singlet parts of $F_{\text{pp}}^{(2)}$, and $F_{\text{ch,sp}}^{(2)}$ the charge and spin parts of $F_{\text{ph}}^{(2)}$. In the next section, we shall use Eq. (67) to reproduce the Ginzburg-Landau expansion of the thermodynamic potential of a BCS superconductor.

III. BCS THEORY

The aim of this section is to reproduce the main results of the BCS theory using the 2PI RG equations. We consider a 3D system described by the action

$$\begin{aligned} S &= \int dx \sum_{\sigma} \psi_{\sigma}^*(x) \left(\partial_{\tau} - \mu - \frac{\nabla_{\mathbf{r}}^2}{2m} \right) \psi_{\sigma}(x) \\ &+ \lambda \int dx \psi_{\uparrow}^*(x) \psi_{\downarrow}^*(x) \psi_{\downarrow}(x) \psi_{\uparrow}(x), \end{aligned} \quad (75)$$

where m is the fermion mass, μ the chemical potential, and $\lambda < 0$ the amplitude of the local attractive interaction. This singular interaction is regularized by means of an ultraviolet cutoff acting on the fermion dispersion: $|\xi_{\mathbf{k}}| < \Lambda_0$, $\xi_{\mathbf{k}} = \mathbf{k}^2/2m - \mu$.

A. BCS gap equation

There are two equivalent ways to derive the RG equations for the BCS theory. One can start from the one-loop equations and neglect the ph channel. Since the one-loop contribution to $\tilde{\Phi}_{\text{pp}}^{(2)}$ involves only the ph channel, it vanishes in the BCS approximation, i.e.

$$\dot{\Phi}_{\text{pp}}^{(2)} = 0. \quad (76)$$

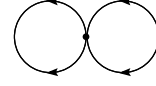


FIG. 6: Luttinger-Ward functional $\Phi_{\text{BCS}}[G]$ in the BCS theory.

Alternatively, one can start directly from the LW functional (Fig. 6)

$$\Phi_{\text{BCS}}[G] = \lambda \int dx G_{\uparrow\downarrow}(x+, x+) G_{\downarrow\uparrow}(x-, x-), \quad (77)$$

where

$$\begin{aligned} G_{\uparrow\downarrow}(x+, x'+) &= \langle \psi_{\uparrow}^*(x) \psi_{\downarrow}^*(x') \rangle, \\ G_{\downarrow\uparrow}(x-, x'-) &= \langle \psi_{\downarrow}(x) \psi_{\uparrow}(x') \rangle. \end{aligned} \quad (78)$$

One then obtain $\Phi_{\gamma_1\gamma_2\gamma_3}^{(3)} = 0$, which leads to Eq. (76).

In the case of a local interaction, the only non-vanishing part of $\Phi_{\text{pp}}^{(2)}$ reads

$$\begin{aligned} \Phi_{\text{pp},\sigma_i}^{(2)}(x_i) &= \tilde{\Phi}_{\text{pp},\sigma_i}^{(2)} \delta(x_1 - x_2) \delta(x_2 - x_3) \delta(x_3 - x_4) \\ \tilde{\Phi}_{\text{pp},\uparrow\downarrow\uparrow}^{(2)} &= -\tilde{\Phi}_{\text{pp},\uparrow\downarrow\downarrow}^{(2)} = -\tilde{\Phi}_{\text{pp},\downarrow\uparrow\downarrow}^{(2)} = \tilde{\Phi}_{\text{pp},\downarrow\uparrow\uparrow}^{(2)} = \lambda, \end{aligned} \quad (79)$$

i.e. $\tilde{\Phi}_{\text{s}}^{(2)} = 2\lambda$ and $\tilde{\Phi}_{\text{t}}^{(2)} = 0$. The self-energy has two non-vanishing elements, $\Sigma_{\uparrow\downarrow}(x+, y+) = -\Sigma_{\downarrow\uparrow}(y+, x+)$ and $\Sigma_{\downarrow\uparrow}(x-, y-) = -\Sigma_{\uparrow\downarrow}(y-, x-)$, determined by the RG equations

$$\begin{aligned} \dot{\Sigma}_{\uparrow\downarrow}(x+, y+) &= \lambda \delta(x - y) \dot{G}_{\downarrow\uparrow}(x-, y-), \\ \dot{\Sigma}_{\downarrow\uparrow}(x-, y-) &= \lambda \delta(x - y) \dot{G}_{\uparrow\downarrow}(x+, y+). \end{aligned} \quad (80)$$

Defining the superconducting order parameter Δ by

$$\begin{aligned} \Sigma_{\uparrow\downarrow}(x+, y+) &= \delta(x - y) \Delta, \\ \Sigma_{\downarrow\uparrow}(x-, y-) &= \delta(x - y) \Delta^*, \end{aligned} \quad (81)$$

the flow equation becomes

$$\dot{\Delta} = \lambda \dot{G}_{\downarrow\uparrow}(x-, x-). \quad (82)$$

Integrating Eq. (82) between Λ_0 and Λ , we obtain the gap equation

$$\Delta = \frac{\lambda}{\beta V} \sum_k G_{\downarrow\uparrow}(k-, k-), \quad (83)$$

where V is the volume of the system, and $k = (\mathbf{k}, i\omega_n)$ with ω_n a fermionic Matsubara frequency.

We use the standard Nambu notation, $\Psi(x) = (\psi_{\uparrow}(x), \psi_{\downarrow}^*(x))^T$, to write the inverse Green function as a 2×2 matrix in reciprocal space,

$$\mathcal{G}^{-1}(k) = \begin{pmatrix} C^{-1}(k) & \Delta \\ \Delta^* & -C^{-1}(-k) \end{pmatrix}, \quad (84)$$

where $C(k)$ is the free propagator defined by Eq. (20). For intermediate calculations, it is convenient to assume that $\Theta_{\mathbf{k}}$ is a smooth cutoff function which does not vanish ($\Theta_{\mathbf{k}} \neq 0$). Final results depend only on $C(k)$ (and not $C^{-1}(k)$) and are well defined even for a hard cutoff $\Theta_{\mathbf{k}} = \Theta(|\xi_{\mathbf{k}}| - \Lambda)$ (Θ is the step function). Inverting \mathcal{G}^{-1} , we obtain

$$\begin{aligned} G_{\sigma\sigma}(k-, k+) &= \Theta_{\mathbf{k}} \frac{i\omega_n + \xi_{\mathbf{k}}}{\omega_n^2 + E_{\mathbf{k}}^2}, \\ G_{\uparrow\downarrow}(k-, k-) &= \Theta_{\mathbf{k}} \frac{\Delta_{\mathbf{k}}}{\omega_n^2 + E_{\mathbf{k}}^2}, \\ G_{\downarrow\uparrow}(k+, k+) &= \Theta_{\mathbf{k}} \frac{\Delta_{\mathbf{k}}^*}{\omega_n^2 + E_{\mathbf{k}}^2}, \end{aligned} \quad (85)$$

where

$$E_{\mathbf{k}} = \sqrt{\xi_{\mathbf{k}}^2 + |\Delta_{\mathbf{k}}|^2}, \quad \Delta_{\mathbf{k}} = \Delta \Theta_{\mathbf{k}}. \quad (86)$$

Using Eqs. (85), we can rewrite the gap equation (83) as

$$\Delta = -\frac{\lambda}{V} \sum_{\mathbf{k}} \frac{\Theta_{\mathbf{k}}^2 \Delta}{2E_{\mathbf{k}}} \tanh\left(\beta \frac{E_{\mathbf{k}}}{2}\right). \quad (87)$$

When $\Delta \neq 0$, this equation becomes

$$\frac{1}{|\tilde{\lambda}|} = \int_{\Lambda}^{\Lambda_0} \frac{d\xi}{\sqrt{\xi^2 + |\Delta|^2}} \tanh\left(\frac{\beta}{2} \sqrt{\xi^2 + |\Delta|^2}\right), \quad (88)$$

where we have taken $\Theta_{\mathbf{k}} = \Theta(|\xi_{\mathbf{k}}| - \Lambda)$. The density of states in the normal phase $N(\xi) = \frac{1}{V} \sum_{\mathbf{k}} \delta(\xi - \xi_{\mathbf{k}})$ has been approximated by its value $N(0)$ at the Fermi level, and $\tilde{\lambda} = N(0)\lambda$ is a dimensionless interaction constant. Eq. (88) can be solved exactly at $T = 0$,

$$|\Delta(T=0)| = |\Delta_0| \left(1 - \frac{2\Lambda}{|\Delta_0|}\right)^{1/2} \Theta\left(\frac{|\Delta_0|}{2} - \Lambda\right), \quad (89)$$

assuming $|\Delta| \ll \Lambda_0$. $|\Delta_0| = |\Delta|_{\Lambda=0} = 2\Lambda_0 e^{1/\tilde{\lambda}}$ is the zero-temperature BCS gap.

When $\Delta(T, \Lambda) = 0$, the singlet response function $\chi_s(x, x, y, y)$ defined in Sec. II E is given by the Bethe-Salpeter equation (59). In Fourier space,

$$\chi_s(q) = \frac{2\Pi^{-+}(q)}{1 + \lambda\Pi^{-+}(q)} \quad (90)$$

($q = (\mathbf{q}, i\omega_\nu)$ with ω_ν a bosonic Matsubara frequency), where $\Pi^{-+}(q)$ is the Fourier transform of the pp propagator

$$\Pi^{-+}(x-y) = [C(x, y)]^2. \quad (91)$$

The condition for $\chi_s(q=0)$ to diverge, $1 + \lambda\Pi^{-+}(q=0) = 0$, is equivalent to the linearized gap equation [Eq. (88) with $\Delta \rightarrow 0^+$].

Fig. 7 shows the superconducting order parameter Δ and the singlet response function $\chi_s(q=0)$ (in the regime

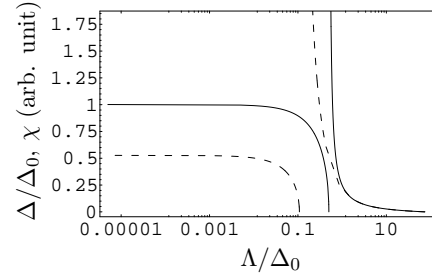


FIG. 7: Order parameter Δ and singlet response function χ_s (for $\Delta(T, \Lambda) = 0$) versus Λ for $T = 0$ (solid lines) and $T = 0.9T_c$ (dashed lines).

where $\Delta(T, \Lambda) = 0$ at $T = 0$ and $T = 0.9T_c$ where T_c is the superconducting transition temperature. χ_s diverges at the threshold value $\Lambda_c(T)$ of the cutoff below which the gap Δ becomes finite and reaches the BCS value for $\Lambda = 0$. The transition temperature is determined by $\Lambda_c(T_c) = 0$. As the 2PI RG equations determine Δ and $\Phi^{(2)}$, they are not plagued with divergencies and can be continued down to $\Lambda = 0$ for any temperature. Broken symmetry is signaled by a finite value of the anomalous self-energy Δ below $\Lambda_c(T)$. The divergence of the singlet response function χ_s is seen only when the 2PI vertex $\Phi^{(2)}$ is fed into the Bethe-Salpeter equation relating χ_s to $\Phi_{pp}^{(2)}$.

Note that we have picked up the nonzero solution of (87) by hand. Alternatively – and this is how one should proceed in more complicated situations – one can directly solve the flow equation (82),⁵⁴

$$\begin{aligned} \frac{\dot{\Delta}}{\tilde{\lambda}} &= \frac{\Delta}{\sqrt{\Lambda^2 + \Delta^2}} \tanh\left(\frac{\beta}{2} \sqrt{\Lambda^2 + \Delta^2}\right) \\ &\quad - \dot{\Delta} \int_{\Lambda}^{\Lambda_0} \frac{d\xi}{E} \tanh\left(\frac{\beta}{2} E\right) \\ &\quad + \dot{\Delta} \Delta^2 \int_{\Lambda}^{\Lambda_0} \frac{d\xi}{E^2} \left[\frac{1}{E} \tanh\left(\frac{\beta}{2} E\right) - \frac{\beta}{2 \cosh^2(\beta E/2)} \right] \end{aligned} \quad (92)$$

($E = \sqrt{\xi^2 + \Delta^2}$ and we assume the gap Δ to be real), together with a symmetry-breaking initial condition $\Delta(\Lambda_0) = \epsilon$. For $\epsilon/\Delta(\Lambda=0) \lesssim 10^{-5}$, the solution of (92) cannot be distinguished from that of (88) when plotted on the same graph. A larger value of ϵ leads to a smearing of the singularity at $\Lambda_c(T)$.

B. Thermodynamic potential

We could determine the thermodynamic potential $\Omega = \beta^{-1}\Gamma$ directly from Eq. (11) using the expression (77) of Φ_{BCS} . To illustrate how the 2PI RG scheme works, we shall instead use the flow equation (25) and the Ginzburg-Landau expansion (67) of the thermodynamic potential near a phase transition.

1. Ground state condensation energy

The ground state condensation energy $\Delta\Omega = \Omega - \Omega_0$ satisfies the RG equation [see Eq. (25)]

$$\begin{aligned}\Delta\dot{\Omega} &= -\frac{1}{2\beta}\text{Tr}[\dot{C}^{-1}(G-C)] \\ &= -\frac{2}{\beta}\sum_k \dot{C}_k^{-1}[G_{\uparrow\uparrow}(k-, k+) - C(k)] \\ &= -\frac{2}{\beta}\sum_k \frac{|\Delta|^2 \dot{\Theta}_k \Theta_k}{\omega_n^2 + E_k^2} \\ &= -|\Delta|^2 \sum_{\mathbf{k}} \frac{\dot{\Theta}_k \Theta_k}{E_k},\end{aligned}\quad (93)$$

where the last line is obtained for $T = 0$. A direct evaluation of this equation by replacing the sum over \mathbf{k} by an integral over $\xi_{\mathbf{k}}$ leads to ambiguities because of factors $\Theta(0)$. We therefore rewrite Eq. (93) as

$$\Delta\dot{\Omega} = -\bar{\partial}_\Lambda \sum_{\mathbf{k}} \sqrt{\xi_{\mathbf{k}}^2 + |\Delta|^2} \Theta_{\mathbf{k}}^2, \quad (94)$$

where $\bar{\partial}_\Lambda$ denotes a derivation with respect to Λ at fixed $|\Delta|$. The calculation is then straightforward and yields

$$\begin{aligned}\Delta\dot{\Omega} &= -2VN(0) \left[\Lambda - \sqrt{\Lambda^2 + |\Delta|^2} \right] \\ &= -2VN(0)(2\Lambda - |\Delta_0|) \Theta\left(\frac{|\Delta_0|}{2} - \Lambda\right),\end{aligned}\quad (95)$$

where we have used Eq. (89). Integrating this equation between Λ_0 and Λ , we finally obtain

$$\Delta\Omega = -2VN(0) \left(\frac{|\Delta_0|}{2} - \Lambda \right)^2 \Theta\left(\frac{|\Delta_0|}{2} - \Lambda\right). \quad (96)$$

For $\Lambda = 0$, we recover the expression of the condensation energy $\Delta\Omega = -\frac{1}{2}VN(0)|\Delta_0|^2$ in a BCS superconductor.

2. Ginzburg-Landau expansion

In the vicinity of the superconducting transition, the thermodynamic potential can be calculated using the general method discussed in Sec. II F. This approach relies on the 2PI RG equations in the normal phase ($\Delta = 0$) continued below the actual transition temperature T_c (i.e. with $\Sigma = \Sigma_N = 0$ and $\Phi^{(2)} = \text{const}$ in the BCS model). The anomalous self-energy $\Delta_{\gamma_1\gamma_2}$ is defined by

$$\begin{aligned}\Delta_{\sigma_1\sigma_2}(x_1c_1, x_2c_2) &= \delta(x_1 - x_2) \delta_{\sigma_1, \sigma_2} \delta_{c_1, c_2} \\ &\quad \times \sigma_1 (\delta_{c_1, +} \Delta - \delta_{c_1, -} \Delta^*).\end{aligned}\quad (97)$$

Using (97), one finds

$$\begin{aligned}\text{Tr}(G_N\Delta)^2 &= -4|\Delta|^2 \sum_k C(k)C(-k) \\ &= -4V\beta|\Delta|^2 N(0) \ln\left(\frac{2\gamma\Lambda_0}{\pi T}\right), \\ \text{Tr}(G_N\Delta)^4 &= 4|\Delta|^4 \sum_k [C(k)C(-k)]^2 \\ &= V\beta|\Delta|^4 \frac{7\zeta(3)N(0)}{2\pi^2 T^2} \\ \frac{1}{8} \sum_{\gamma_1, \gamma_2} F_{\gamma_1\gamma_2}^{(2)} \Delta_{\gamma_1} \Delta_{\gamma_2} &= \frac{|\Delta|^2}{2} \int dx_1 dx_2 F_s^{(2)}(x_1, x_1, x_2, x_2) \\ &= -V\beta \frac{|\Delta|^2}{\lambda},\end{aligned}\quad (98)$$

where $\gamma \simeq 1.78$ is the exponential of the Euler constant and $\zeta(z)$ the Riemann zeta function ($\zeta(3) \simeq 1.2$). To obtain the last line, we have used the relation (74) between $\Phi_s^{(2)}$ and $F_s^{(2)}$ and Eq. (79). From Eqs. (67,98), we recover the Ginzburg-Landau expansion in a BCS superconductor,

$$\frac{\Delta\Omega}{V} = |\Delta|^2 \left[\frac{1}{|\lambda|} - N(0) \ln\left(\frac{2\gamma\Lambda_0}{\pi T}\right) \right] + \frac{7\zeta(3)N(0)}{16\pi^2 T^2} |\Delta|^4. \quad (99)$$

C. Response function and collective modes in the superconducting phase

For $\Lambda < \Lambda_c(T)$, where $\Delta(T, \Lambda) \neq 0$, the singlet superconducting response function is defined by

$$\begin{aligned}\chi_s^{c_1c_2}(x_1, x_2) &= \frac{1}{2} \sum_{\sigma_1, \sigma_2} \sigma_1 \bar{\sigma}_2 \\ &\quad \times W_{\sigma_1 \bar{\sigma}_1 \sigma_2 \bar{\sigma}_2}^{(2)}(x_1, c_1, x_1, c_1, x_2, c_2, x_2, c_2).\end{aligned}\quad (100)$$

Using the Bethe-Salpeter equation (17), we obtain

$$\begin{aligned}\chi_s^{-+}(q) &= 2\Pi^{-+}(q) - \lambda\Pi^{-+}(q)\chi_s^{-+}(q) \\ &\quad - \lambda\Pi^{--}(q)\chi_s^{++}(q), \\ \chi_s^{++}(q) &= 2\Pi^{++}(q) - \lambda\Pi^{+-}(q)\chi_s^{++}(q) \\ &\quad - \lambda\Pi^{++}(q)\chi_s^{-+}(q),\end{aligned}\quad (101)$$

where $\Pi^{c_1c_2}(q)$ is the Fourier transform of

$$\begin{aligned}\Pi^{-+}(x-y) &= \Pi^{+-}(y-x) = G_{\uparrow\uparrow}(x, y)G_{\downarrow\downarrow}(x, y), \\ \Pi^{--}(x-y) &= -G_{\downarrow\uparrow}(x-, y-)G_{\uparrow\downarrow}(x-, y-), \\ \Pi^{++}(x-y) &= -G_{\uparrow\downarrow}(x+, y+)G_{\downarrow\uparrow}(x+, y+).\end{aligned}\quad (102)$$

Collective modes are obtained from the poles of $\chi^{c_1c_2}(q)$,

$$[1 + \lambda\Pi^{-+}(q)][1 + \lambda\Pi^{+-}(q)] - \lambda^2\Pi^{++}(q)\Pi^{--}(q) = 0. \quad (103)$$

Using

$$\begin{aligned}
\Pi^{+-}(q=0) &= \Pi^{+-(q=0)} \\
&= -\frac{1}{\lambda} - \frac{1}{\beta V} \sum_k \frac{\Theta_k^2 |\Delta_k|^2}{(\omega_n^2 + E_k^2)^2}, \\
\Pi^{--}(q=0) &= \Pi^{++}(q=0)^* \\
&= \frac{1}{\beta V} \sum_k \frac{\Delta_k^2}{(\omega_n^2 + E_k^2)^2}, \tag{104}
\end{aligned}$$

one verifies that Eq. (103) is satisfied for $\mathbf{q} = 0$ and $\omega_\nu = 0$. For any finite value of the gap Δ (i.e. for $\Lambda < \Lambda_c$), we therefore obtain a gapless (Goldstone) mode (Anderson-Bogoliubov mode^{55,56}). Note that the Goldstone theorem is ensured by the fact that the BCS theory is a Φ -derivable approximation.

IV. ONE-DIMENSIONAL SYSTEMS

In this section, we consider a 1D system with the action (for a review on 1D systems, see Ref. 12)

$$\begin{aligned}
S_0 &= - \sum_{k,r,\sigma} \psi_{r\sigma}^*(k) [i\omega_n - \xi_r(k_\parallel)] \psi_{r\sigma}(k), \\
S_{\text{int}} &= \frac{1}{2\beta L} \sum_{\substack{k,k',q \\ r,r',\sigma,\sigma'}} (g_2 \delta_{r,r'} + g_1 \delta_{r,\bar{r}'}) \\
&\quad \times \psi_{r\sigma}^*(k+q) \psi_{\bar{r}'\sigma'}^*(k'-q) \psi_{\bar{r}'\sigma'}(k') \psi_{r\sigma}(k) \tag{105}
\end{aligned}$$

where L is the length of the system, $k = (k_\parallel, i\omega_n)$, and $q = (q_\parallel, i\omega_\nu)$. k_\parallel and q_\parallel denote momenta, ω_n and ω_ν fermionic and bosonic Matsubara frequencies, respectively. The index r distinguishes between right ($r = +$) and left ($r = -$) moving fermions. $\xi_r(k_\parallel) = \epsilon_r(k_\parallel) - \mu = v_F(rk_\parallel - k_F)$ is the dispersion law, linearized around the two Fermi points $\pm k_F$, μ being the chemical potential. The bandwidth is $2\Lambda_0 = 2\max|\xi_r(k_\parallel)|$. g_1 and g_2 are the backward and forward scattering amplitudes, respectively. We assume the band filling to be incommensurate and neglect Umklapp processes.

A. One-loop RG equations

The 2PI two-particle vertex $\Phi_{\text{pp,ph}}^{(2)r_1 r_2 r_3 r_4}(X_i)$ now carries left/right indices r_i . Momentum conservation implies $\sum_i r_i = 0$. We define

$$\begin{aligned}
\Phi_\mu^{\text{C}}(x_i) &= \Phi_\mu^{(2)++++}(x_i), \quad (\mu = \text{t, s}), \\
\Phi_\mu^{\text{P}}(x_i) &= \Phi_\mu^{(2)++--}(x_i), \quad (\mu = \text{ch, sp}), \\
\Phi_\mu^{\text{L}}(x_i) &= \Phi_\mu^{(2)++--}(x_i), \quad (\mu = \text{ch, sp}), \tag{106}
\end{aligned}$$

where C, P, and L refer to the Cooper, Peierls, and Landau channels according to the standard terminology used

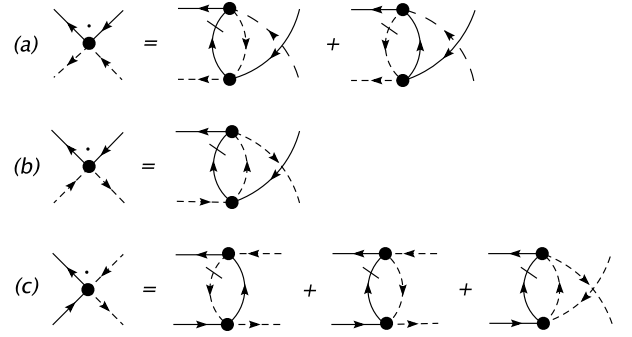


FIG. 8: One-loop RG equations for the 2PI vertex $\Phi^{(2)}$ in the Cooper (a), Peierls (b) and Landau (c) channels in a 1D system. Solid and dashed lines indicate right- and left-moving fermions, respectively. [In the pp loops appearing in (b) and (c), a sum over the left/right indices is implied.]

in the framework of the g-ology model.¹² In Fourier space, we neglect the frequency dependence and approximate

$$\begin{aligned}
\Phi_\mu^{\text{C}}(k_1, k_2, k_3, k_4) &\simeq \Phi_\mu^{\text{C}}(k_F, -k_F, -k_F, k_F) \equiv \Phi_\mu^{\text{C}}, \\
\Phi_\mu^{\text{P}}(k_1, k_2, k_3, k_4) &\simeq \Phi_\mu^{\text{P}}(k_F, -k_F, -k_F, k_F) \equiv \Phi_\mu^{\text{P}}, \\
\Phi_\mu^{\text{L}}(k_1, k_2, k_3, k_4) &\simeq \Phi_\mu^{\text{L}}(k_F, k_F, -k_F, -k_F) \equiv \Phi_\mu^{\text{L}}. \tag{107}
\end{aligned}$$

By scaling arguments, one can show that the dependence of the 1PI vertex $\gamma^{(4)}(k_i)$ on ω_{n_i} and $|k_{i\parallel}| - k_F$ is irrelevant in the RG sense. The validity of Eq. (107), which assumes that the 2PI vertex $\Phi^{(2)}$ shares the same property, will be discussed in Sec. IV C. One-loop flow equations for Φ^{C} , Φ^{P} and Φ^{L} are deduced from Eqs. (54) by including the r index, i.e. $x_i \rightarrow (x_i, r_i)$. Retaining only leading logarithmic divergent loops (Parquet approximation),¹² the contribution to the self-energy vanishes and the RG equations for the two-particle vertex read (see Fig. 8)

$$\begin{aligned}
\dot{\Phi}_{\text{t}}^{\text{C}} &= -B_{\text{ph}} (\Phi_{\text{t}}^{\text{C}} \Phi_{\text{ch}}^{\text{L}} + 2\Phi_{\text{t}}^{\text{C}} \Phi_{\text{sp}}^{\text{L}} - \Phi_{\text{s}}^{\text{C}} \Phi_{\text{sp}}^{\text{L}}), \\
\dot{\Phi}_{\text{s}}^{\text{C}} &= -B_{\text{ph}} (\Phi_{\text{s}}^{\text{C}} \Phi_{\text{ch}}^{\text{L}} - 3\Phi_{\text{t}}^{\text{C}} \Phi_{\text{sp}}^{\text{L}}), \\
\dot{\Phi}_{\text{ch}}^{\text{P}} &= -B_{\text{pp}} (\Phi_{\text{ch}}^{\text{P}} \Phi_{\text{ch}}^{\text{L}} + 3\Phi_{\text{sp}}^{\text{P}} \Phi_{\text{sp}}^{\text{L}}), \\
\dot{\Phi}_{\text{sp}}^{\text{P}} &= -B_{\text{pp}} (\Phi_{\text{ch}}^{\text{P}} \Phi_{\text{sp}}^{\text{L}} + \Phi_{\text{sp}}^{\text{P}} \Phi_{\text{ch}}^{\text{L}} - 2\Phi_{\text{sp}}^{\text{P}} \Phi_{\text{sp}}^{\text{L}}), \\
\dot{\Phi}_{\text{ch}}^{\text{L}} &= -\frac{1}{2} B_{\text{ph}} \left(\frac{3}{4} \Phi_{\text{t}}^{\text{C}2} + \frac{1}{4} \Phi_{\text{s}}^{\text{C}2} + \Phi_{\text{ch}}^{\text{L}2} + 3\Phi_{\text{sp}}^{\text{L}2} \right) \\
&\quad - \frac{1}{2} B_{\text{pp}} \left(\Phi_{\text{ch}}^{\text{L}2} + 3\Phi_{\text{sp}}^{\text{L}2} + \Phi_{\text{ch}}^{\text{P}2} + 3\Phi_{\text{sp}}^{\text{P}2} \right), \\
\dot{\Phi}_{\text{sp}}^{\text{L}} &= -B_{\text{ph}} \left(\frac{1}{4} \Phi_{\text{t}}^{\text{C}2} - \frac{1}{4} \Phi_{\text{t}}^{\text{C}} \Phi_{\text{s}}^{\text{C}} + \Phi_{\text{ch}}^{\text{L}} \Phi_{\text{sp}}^{\text{L}} + \Phi_{\text{sp}}^{\text{L}2} \right) \\
&\quad - B_{\text{pp}} \left(\Phi_{\text{ch}}^{\text{L}} \Phi_{\text{sp}}^{\text{L}} - \Phi_{\text{sp}}^{\text{L}2} + \Phi_{\text{ch}}^{\text{P}} \Phi_{\text{sp}}^{\text{P}} - \Phi_{\text{sp}}^{\text{P}2} \right), \tag{108}
\end{aligned}$$

where

$$\begin{aligned}
B_{\text{ph}} &= \frac{1}{\beta L} \sum_k [G_+(k) \dot{G}_-(k-Q) + (G \leftrightarrow \dot{G})], \\
B_{\text{pp}} &= \frac{1}{\beta L} \sum_k [G_+(k) \dot{G}_-(-k) + (G \leftrightarrow \dot{G})] \tag{109}
\end{aligned}$$

come from the ph and pp loops, and $Q = (2k_F, 0)$. The dot denotes a derivation with respect to $l = \ln(\Lambda_0/\Lambda)$. To evaluate B_{ph} and B_{pp} , we use a sharp infrared cutoff,

$$G_r(k) = C_r(k) = -\frac{\Theta(|\xi_r(k_{\parallel})| - \Lambda)}{i\omega_n - \xi_r(k_{\parallel})}. \quad (110)$$

This gives

$$B_{\text{pp}} = -B_{\text{ph}} = \frac{1}{2\pi v_F} \tanh\left(\beta\frac{\Lambda}{2}\right). \quad (111)$$

The initial values of the 2PI vertex $\Phi^{(2)}$ is the bare vertex defined by Eq. (105),

$$\begin{aligned} \Phi_{\text{t}}^{\text{C}}|_{\Lambda_0} &= -g_1 + g_2, & \Phi_{\text{s}}^{\text{C}}|_{\Lambda_0} &= g_1 + g_2, \\ \Phi_{\text{ch}}^{\text{P}}|_{\Lambda_0} &= g_1 - \frac{g_2}{2}, & \Phi_{\text{sp}}^{\text{P}}|_{\Lambda_0} &= -\frac{g_2}{2}, \\ \Phi_{\text{ch}}^{\text{L}}|_{\Lambda_0} &= -\frac{g_1}{2} + g_2, & \Phi_{\text{sp}}^{\text{L}}|_{\Lambda_0} &= -\frac{g_1}{2}. \end{aligned} \quad (112)$$

B. Response functions and 1PI vertices

The response functions in the Cooper and Peierls channels are defined by

$$\begin{aligned} \chi_{\text{t,s}}^{\text{C}} &= \frac{1}{\beta L} \sum_{k,k'} \chi_{\text{t,s}}^{+---}(k, -k, -k', k'), \\ \chi_{\text{ch,sp}}^{\text{P}} &= \frac{1}{\beta L} \sum_{k,k'} \chi_{\text{ch,sp}}^{+---}(k, k - Q, k' - Q, k'). \end{aligned} \quad (113)$$

From the Bethe-Salpeter equations satisfied by $\chi_{\text{t,s}}^{+---}$ and $\chi_{\text{ch,sp}}^{+---}$ (Eqs. (59) with the r_i index included), we obtain

$$\begin{aligned} \chi_{\mu}^{\text{C}} &= \frac{\Pi_{\text{pp}}}{1 + \Pi_{\text{pp}}\Phi_{\mu}^{\text{C}}}, \\ \chi_{\mu}^{\text{P}} &= \frac{-2\Pi_{\text{ph}}}{1 - 2\Pi_{\text{ph}}\Phi_{\mu}^{\text{P}}}, \end{aligned} \quad (114)$$

where

$$\begin{aligned} \Pi_{\text{pp}} &= \frac{1}{\beta L} \sum_k G_+(k)G_-(-k) \\ &= \frac{1}{2\pi v_F} \int_{\Lambda}^{\Lambda_0} \frac{d\xi}{\xi} \tanh\left(\beta\frac{\xi}{2}\right), \\ \Pi_{\text{ph}} &= \frac{1}{\beta L} \sum_k G_+(k)G_-(k - Q) \\ &= -\Pi_{\text{pp}}. \end{aligned} \quad (115)$$

Similarly, for the 1PI two-particle vertex $\gamma^{(4)}$ [Eq. (61)], we find

$$\begin{aligned} \gamma_{\mu}^{\text{C}} &= \frac{\Phi_{\mu}^{\text{C}}}{1 + \Pi_{\text{pp}}\Phi_{\mu}^{\text{C}}}, \\ \gamma_{\mu}^{\text{P}} &= \frac{\Phi_{\mu}^{\text{P}}}{1 - 2\Pi_{\text{ph}}\Phi_{\mu}^{\text{P}}}, \\ \gamma_{\mu}^{\text{L}} &= \Phi_{\mu}^{\text{L}}. \end{aligned} \quad (116)$$

The equality between γ_{μ}^{L} and Φ_{μ}^{L} is due to the absence of logarithmic divergent loops in the Landau channel and holds at the Parquet level.

In Sec. II, we have shown very generally that the RG equation for $\gamma^{(4)}$ derived within the 1PI scheme follows from the RG equation satisfied by the 2PI vertex $\Phi^{(2)}$ and the Bethe-Salpeter equation relating $\gamma^{(4)}$ and $\Phi^{(2)}$. In appendix A, as a means to check the validity of Eqs. (108), we recover the RG equation satisfied by $\gamma^{(4)}$ directly from Eqs. (108,116).

C. Discussion

Figure 9 shows $\Phi^{(2)}$, χ and $\gamma^{(4)}$ versus $l = \ln(\Lambda_0/\Lambda)$ at zero temperature for $\tilde{g}_1 = \tilde{g}_2 = 0.2$. $\tilde{g}_1 = g_1/\pi v_F$ and $\tilde{g}_2 = g_2/\pi v_F$ are dimensionless coupling constants. Solid lines show the results obtained within the 2PI scheme by solving the flow equations (108) and using Eqs. (114,116). Dashed lines correspond to results obtained within the 1PI scheme, where $\gamma^{(4)}$ and χ are directly obtained from RG equations, the 2PI vertex $\Phi^{(2)}$ being then deduced from the relations (116). The agreement between the two schemes is excellent at high energies (small l), but deteriorates at lower energies where, in at least one correlation channel, the 2PI vertex $\Phi^{(2)}$ becomes of order one and eventually diverges. This deficiency is not important in the 1PI scheme, as $\Phi^{(2)}$ is usually not considered in this scheme, but it shows that the one-loop approximation breaks down in the 2PI scheme at low energy.

The divergence of the 2PI vertex $\Phi^{(2)}$ in the 1PI scheme, which correctly predicts all other physical quantities, suggests that the relations (116) between 1PI and 2PI vertices may not be quite correct. Inverting Eqs. (116) and considering the zero temperature limit, we obtain $\tilde{\Phi}_{\mu}^{\text{C}}(l) = \tilde{\gamma}_{\mu}^{\text{C}}(l)/(1 - l\tilde{\gamma}_{\mu}^{\text{C}}/2)$ in the Cooper channel and $\tilde{\Phi}_{\mu}^{\text{P}}(l) = \tilde{\gamma}_{\mu}^{\text{P}}(l)/(1 - l\tilde{\gamma}_{\mu}^{\text{P}})$ in the Peierls channel. $\tilde{\Phi} = \Phi/\pi v_F$ and $\tilde{\gamma} = \gamma/\pi v_F$ are dimensionless vertices. We conclude that the 2PI vertex $\Phi^{(2)}$ will diverge at a finite energy scale $\Lambda_c = \Lambda_0 e^{-l_c}$ whenever $\gamma^{(4)}$ is positive and finite in the low-energy limit ($l \rightarrow \infty$). For repulsive interactions, $\gamma_s^{\text{C}}(l) \rightarrow g_2 - g_1/2$ satisfies this condition when $g_2 > g_1/2$, which leads to the divergence of the 2PI vertex Φ_s^{C} (see Fig. 9). The unphysical divergence of the 2PI vertex $\Phi^{(2)}$ comes from the assumption that the 2PI vertex is momentum independent [Eq. (107)], which results in an artificial decoupling of energy scales between the 2PI vertex and the reducible pp (or ph) propagator $\Pi_{\text{pp,ph}}$. The latter involves all energy scales between Λ and Λ_0 whereas the momentum-independent $\Phi^{(2)}$ is an effective 2PI vertex at the energy scale Λ . The Bethe-Salpeter equations (114) and (116) are therefore expected to be less and less reliable as the infrared cutoff Λ decreases.

These difficulties can be partially overcome by modifying the Bethe-Salpeter equation relating $\Phi^{(2)}$ to $\gamma^{(4)}$ and

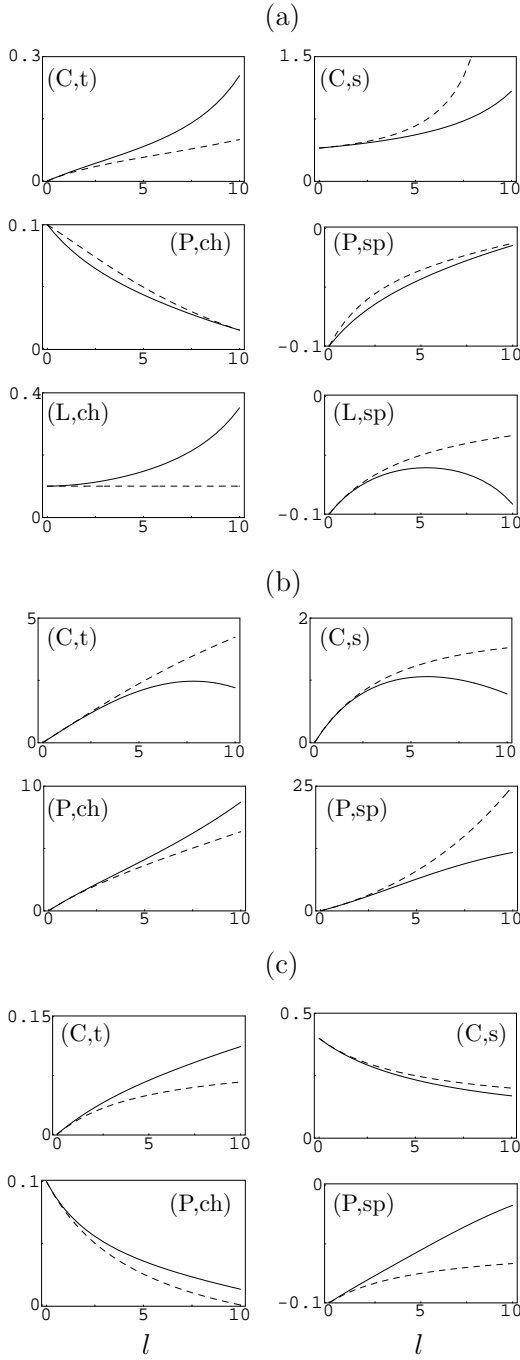


FIG. 9: 2PI vertices $\Phi^{(2)}$ (a), response functions χ (b) and 1PI vertices $\gamma^{(4)}$ (c) versus $l = \ln(\Lambda_0/\Lambda)$ for $\tilde{g}_1 = \tilde{g}_2 = 0.2$ and $T = 0$. Units are chosen such that $\pi\nu_F = 1$. The correlation channel is indicated in the upper left or right corner of each graph, following the notation of the text: (C,t)=(Cooper,triplet), etc. The solid (dashed) lines show the results obtained from the 2PI (1PI) RG scheme. In the 1PI RG scheme, the 2PI vertex $\Phi^{(2)}$ (dashed lines in panel (a)) is deduced from $\gamma^{(4)}$ using the relations (116).

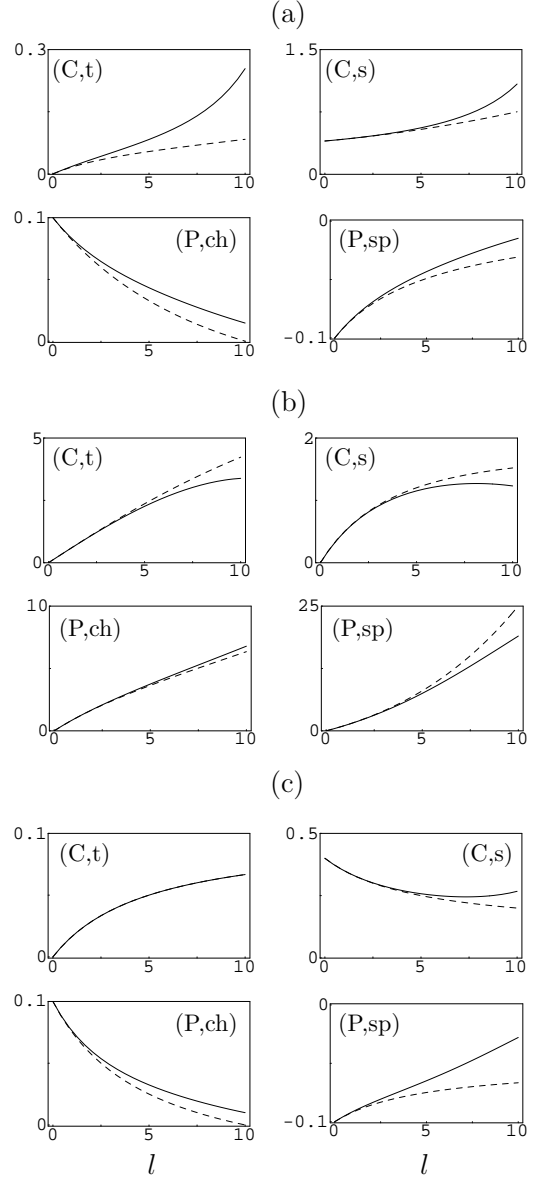


FIG. 10: Same as Fig. 9, but using Eqs. (118) instead of Eqs. (114,116).

χ ,

$$\begin{aligned}
 \tilde{\gamma}_\mu^C(\Lambda) &= \tilde{\Phi}_\mu^C(\Lambda) - \frac{1}{2} \int_\Lambda^{\Lambda_0} \frac{d\xi}{\xi} \tanh\left(\beta \frac{\xi}{2}\right) \tilde{\Phi}_\mu^C(\Lambda) \tilde{\gamma}_\mu^C(\Lambda) \\
 &\rightarrow \tilde{\Phi}_\mu^C(\Lambda) - \frac{1}{2} \int_\Lambda^{\Lambda_0} \frac{d\xi}{\xi} \tanh\left(\beta \frac{\xi}{2}\right) \tilde{\Phi}_\mu^C(\xi) \tilde{\gamma}_\mu^C(\Lambda), \\
 \chi_\mu^C(\Lambda) &= \Pi_{pp}(\Lambda) - \frac{1}{2} \int_\Lambda^{\Lambda_0} \frac{d\xi}{\xi} \tanh\left(\beta \frac{\xi}{2}\right) \tilde{\Phi}_\mu^C(\Lambda) \chi_\mu^C(\Lambda) \\
 &\rightarrow \Pi_{pp}(\Lambda) - \frac{1}{2} \int_\Lambda^{\Lambda_0} \frac{d\xi}{\xi} \tanh\left(\beta \frac{\xi}{2}\right) \tilde{\Phi}_\mu^C(\xi) \chi_\mu^C(\Lambda),
 \end{aligned} \tag{117}$$

and similar equations in the ph channel. The 2PI vertex $\Phi^{(2)}$ is now taken at the same energy scale than the pp

or ph propagator. We thus obtain

$$\begin{aligned}\gamma_\mu^C &= \frac{\Phi_\mu^C}{1 + \frac{\tilde{\Psi}_\mu^C}{2}}, & \chi_\mu^C &= \frac{\Pi_{pp}}{1 + \frac{\tilde{\Psi}_\mu^C}{2}}, \\ \gamma_\mu^P &= \frac{\Phi_\mu^P}{1 + \tilde{\Psi}_\mu^P}, & \chi_\mu^P &= \frac{-2\Pi_{ph}}{1 + \tilde{\Psi}_\mu^P},\end{aligned}\quad (118)$$

where

$$\Psi_\mu^{C,P} = \int_\Lambda^{\Lambda_0} \frac{d\xi}{\xi} \tanh\left(\beta \frac{\xi}{2}\right) \Phi_\mu^{C,P} \Big|_{\Lambda=\xi} \quad (119)$$

satisfies the flow equation

$$\dot{\Psi}_\mu^{C,P} = \tanh\left(\beta \frac{\Lambda}{2}\right) \Phi_\mu^{C,P}. \quad (120)$$

Fig. 10 shows $\Phi^{(2)}$, χ and $\gamma^{(4)}$ obtained from Eqs. (118) instead of Eqs. (114,116). The parameters are the same as in Fig. 9. We see that the agreement between the 1PI and 2PI schemes, in particular for the susceptibilities, is significantly better. It is instructive to consider the case $g_1 = 0$ where the 1PI vertices γ_μ^C and γ_μ^P are fixed points of the flow equations at any order in a loop expansion. From Eqs. (118,120), one then obtains $\Phi_\mu^C = \Phi_\mu^C(l=0) \exp(\frac{1}{2}\tilde{\gamma}_\mu^C l)$ and $\Phi_\mu^P = \Phi_\mu^P(l=0) \exp(\tilde{\gamma}_\mu^P l)$ at zero temperature. Depending on the sign of γ_μ , the 2PI vertex will either vanish or diverge exponentially in the limit $l \rightarrow \infty$. The unphysical divergence of the 2PI vertex obtained earlier at a finite energy scale is now replaced by an exponential divergence at zero energy ($\Lambda = \Lambda_0 e^{-l} \rightarrow 0$). This divergence follows from the coexistence of logarithmically divergent (reducible) pp and ph loops and weak 1PI vertices, which is made possible in 1D by the strong interferences between various correlation channels. The 2PI flow equations give the correct qualitative behavior of $\Phi^{(2)}$, but the one-loop approximation clearly breaks down at low energy when $\Phi^{(2)}$ becomes of order one.

It should be noticed that if, within the 1PI scheme, the susceptibilities were calculated from

$$\begin{aligned}\chi_\mu^C &= \Pi_{pp} - \Pi_{pp} \gamma_\mu^C \Pi_{pp}, \\ \chi_\mu^P &= -2\Pi_{ph} - 4\Pi_{ph} \gamma_\mu^P \Pi_{ph},\end{aligned}\quad (121)$$

with momentum independent vertices $\gamma^{(4)}$ obtained from RG equations, similar difficulties would arise and the correct asymptotic low-energy behavior would not be reached. The correct result is obtained by also deriving RG equations for the susceptibilities; in this way irreducible and reducible pp and ph loops are considered on equal footing. These RG equations are obtained by introducing bosonic external sources that couple to order parameter fields, in addition to the fermionic sources that are used to obtain the generating functional of 1PI vertices by a Legendre transformation.^{23,25}

To quantify the failure of the 2PI scheme, within the one-loop approximation, to access the low-energy limit

of 1D systems, let us consider the case of the quasi-1D organic conductors of the Bechgaard salt family. In these systems, the bandwidth $2\Lambda_0 \simeq 4t_{\parallel} \sim 12000$ K is much larger than the kinetic interchain coupling $t_{\perp} \sim 300$ K. For $\tilde{g}_1 = \tilde{g}_2 = 0.2$, the 2PI flow equations break down for $l \sim 5$ (Fig. 10), which corresponds to an energy or temperature scale $\Lambda_0 e^{-l} \sim 40$ K. For $\tilde{g}_1 = \tilde{g}_2 = 0.4$, we find that the flow equations remain valid down to $\sim \Lambda_0 e^{-3} \sim 300$ K. In both cases, these energy scales are of the same order of magnitude or smaller than the temperature $T_x \sim t_{\perp} \sim 300$ K at which a crossover to a 2D regime takes place. Preliminary calculations in quasi-1D systems indicate that the interaction strength studied in Refs. 15,16, namely $\tilde{g}_2 = 2\tilde{g}_1 = 0.64$ is accessible within the 2PI scheme.⁵⁷ We thus conclude that the 2PI scheme can be used for realistic quasi-1D systems like the Bechgaard salts.

V. SUMMARY AND CONCLUSION

We have discussed the implementation of a Wilsonian momentum-shell RG approach within the 2PI formalism introduced in the 60s by Luttinger, Ward, Baym and others.^{1,2,3,4} The 2PI RG scheme yields an infinite hierarchy of flow equations satisfied by the 2PI vertices $\Phi^{(n)}$. The susceptibilities are obtained from the Bethe-Salpeter equation that relates them to the 2PI two-particle vertex $\Phi^{(2)}$. In the normal phase, one has schematically

$$\begin{aligned}\chi_{pp} &= \chi_{pp}^{(0)} - \frac{1}{2}\Pi_{pp}\Phi_{pp}^{(2)}\chi_{pp} \\ &\quad \uparrow \\ &\quad \text{(RG equations)} \\ &\quad \downarrow \\ \chi_{ph} &= \chi_{ph}^{(0)} + 2\Pi_{ph}\Phi_{ph}^{(2)}\chi_{ph}\end{aligned}$$

(similar equations could be written for the 1PI vertices $\gamma_{pp}^{(4)}$ and $\gamma_{ph}^{(4)}$) where $\chi_{pp,ph}^{(0)}$ are the susceptibilities without vertex correction and $\Pi_{pp/ph}$ the pp or ph pair propagator. The arrows indicate the coupling between the pp and ph channels which is taken care of by the RG equations satisfied by the 2PI two-particle vertices $\Phi_{pp}^{(2)}$ and $\Phi_{ph}^{(2)}$. The infinite hierarchy of RG flow equations satisfied by the 2PI vertices $\Phi^{(n)}$ should be truncated at some order in a loop expansion. The simplest non trivial truncation, the one-loop approximation, was discussed in detail in Sec. II. As any approximation of the 2PI vertex $\Phi^{(2)}$, it leads to a violation of the crossing symmetries of the two-particle Green function $W^{(2)}$ and the 1PI vertex $\gamma^{(4)}$. Besides, the one-loop approximation is not a Φ -derivable approximation, and a detailed study of conservation laws and Ward identities remains to be done.

We have shown in Sec. IV that 1D conductors are characterized by an exponentially divergent 2PI vertex in the zero-energy limit, a consequence of the strong interferences between correlation channels in 1D. This leads to a breakdown of the one-loop approximation, which is there-

fore unable to access the asymptotic low-energy behavior of Luttinger liquids. Nevertheless, we have argued that the 2PI scheme can be used in quasi-1D systems like the organic conductors of the Bechgaard family where a dimensional crossover always drives the system towards a 2D or 3D behavior at low energy.

On the other hand, the 2PI RG scheme leads to a particularly simple description of single-channel (i.e. mean-field) theories. In mean-field theories, all the Λ dependence comes from the two-particle-reducible part of the susceptibilities (and the 1PI vertex $\gamma^{(4)}$), while the 2PI vertex $\Phi^{(2)}$ is invariant under the RG transformation: $\dot{\Phi}^{(2)} = 0$. The one-loop flow equations then reduce to a single equation that determines the (anomalous) self-energy and reproduces the usual mean-field gap equation (Sec. III).

The possibility to continue the RG flow into broken-symmetry phases is an essential feature of the 2PI RG scheme and is due to the fact that the 2PI two-particle vertex $\Phi^{(2)}$, contrary to its 1PI counterpart, is not singular at the phase transition. This property, which is obvious in a mean-field theory, deserves some discussion in more general cases. The interchannel coupling, even weak, is likely to induce singularities in the 2PI vertex $\Phi^{(2)}$, in particular in the vicinity of a phase transition. However, these singularities can be controlled by a proper parameterization of $\Phi^{(2)}$. To see this, let us consider a quasi-1D conductor near a spin-density-wave (SDW) instability. The spin susceptibility $\chi_{\text{sp}}(2k_F, \pi)$ diverges at the SDW transition but, as in single-channel (mean-field) theories, the irreducible vertex $\Phi_{\text{sp}}^{\text{P}}$ should remain finite (see Sec. IV for the definition of Φ^{P} and Φ^{C} in a (quasi)-1D system). In the vicinity of the phase transition, nearly divergent spin fluctuations strongly affect the 2PI vertex Φ^{C} in the Cooper channel. For the purpose of our discussion, let us assume that Φ^{C} is proportional to the spin susceptibility,

$$\Phi_{\mu=\text{t,s}}^{\text{C}}(k_{\perp}, q_{\perp} - k_{\perp}, -k'_{\perp}, k'_{\perp} - q_{\perp}) \propto \chi_{\text{sp}}(2k_F, k_{\perp} + k'_{\perp}), \quad (122)$$

where we retain the k_{\perp} dependence of the vertex.¹⁶ The combination of k_{\perp} arguments in Eq. (122) is the one that appears in the Bethe-Salpeter equation determining the superconducting susceptibility. Expanding the even function $\chi_{\text{sp}}(2k_F, q_{\perp})$ in Fourier series, we obtain

$$\begin{aligned} \Phi_{\mu}^{\text{C}}(k_{\perp}, q_{\perp} - k_{\perp}, -k'_{\perp}, k'_{\perp} - q_{\perp}) &= \sum_{n=0}^{\infty} a_{\mu}^{(n)} \cos[n(k_{\perp} + k'_{\perp})] \\ &= \sum_{n=0}^{\infty} a_{\mu}^{(n)} [\cos(nk_{\perp}) \cos(nk'_{\perp}) - \sin(nk_{\perp}) \sin(nk'_{\perp})], \end{aligned} \quad (123)$$

where $a_{\mu}^{(n+1)} a_{\mu}^{(n)} < 0$ and $|a_{\mu}^{(n)}|$ is a decreasing function of n . The condition $|a_{\mu}^{(n)}| = |a_{\mu}^{(0)}|$, i.e. $a_{\mu}^{(n)} = (-1)^n a_{\mu}^{(0)}$, would lead to a diverging susceptibility $\chi_{\text{sp}}(2k_F, q_{\perp}) \propto$

$\delta(q_{\perp} - \pi)$, while $|a_{\mu}^{(n+1)}| < |a_{\mu}^{(n)}|$ gives a broadened peak at $q_{\perp} = \pi$. The proximity of the SDW transition manifests itself by a larger and larger number of $a_{\mu}^{(n)}$ coefficients with a significant amplitude. All these coefficients should however remain bounded, with $1 \pm (a_{\mu}^{(n)}/2)\Pi_{\text{pp}} > 0$, for the system to be stable against a superconducting instability (Π_{pp} is the pp propagator defined in (115)). By parameterizing the 2PI vertex Φ^{C} by means of the $a_{\mu}^{(n)}$ coefficients, we avoid any complication due to the diverging spin susceptibility. In practice, only a finite number of coefficients need to be retained. The coefficients with a large value of n , which correspond to pairing between fermions n chain apart, do not play an important role; they cannot drive a pairing instability – an instability with a small value of n ($n = 0, 1, 2, \dots$) will always occur first⁵⁸ – and their influence on the ph channel is expected to be negligible. This approximation will lead to a non essential smearing of the singularity of Φ_{μ}^{C} at $k_{\perp} + k'_{\perp} = \pi$. The argument given here for quasi-1D systems can be made more general. One can expand the 2PI vertex on the eigenmodes of the Bethe-Salpeter equation, retaining only a finite number of eigenmodes. Each coefficient in this expansion is bounded by a critical value at which a phase transition occurs.

In Sec. II F, we have proposed a method to derive the Ginzburg-Landau expansion of the thermodynamic potential in the vicinity of the phase transition on the basis of the flow equations in the normal phase. This is the simplest way to access phases with long-range order as it does not require to solve the full RG equations in the presence of symmetry breaking. The knowledge of the Ginzburg-Landau expansion of the thermodynamic potential allows one to study the possibility of phase coexistence below the transition temperature. This is a particularly important issue in quasi-1D organic conductors where superconductivity and antiferromagnetism,^{59,60} as well as spin- and charge-density waves,^{61,62} coexist in some regions of the pressure-temperature phase diagram. Recent 1PI RG calculations have indicated that antiferromagnetism and superconductivity, as well as charge- and spin-density-wave phases, lie nearby in the phase diagram of quasi-1D conductors.^{13,14,15,16} The 2PI RG scheme would allow to determine whether they actually coexist in the low-temperature phase as observed experimentally.^{59,60,61,62}

Finally, we note that the 2PI RG scheme enables a direct connection to the phenomenological Landau Fermi liquid theory when the metallic state remains stable down to low temperature. It has been shown in Ref. 63 that the functional $\Gamma[\bar{G}]$, or rather its variation $\delta\Gamma = \Gamma[G] - \Gamma[\bar{G}]$, can be written as a functional $\delta\Gamma[\delta n]$ of the Wigner distribution function $n = \{n_{\mathbf{k}\sigma}(\mathbf{r}, \tau)\}$ which is essentially determined by the Landau parameters. The latter are given by the forward-scattering limit of the 2PI vertex $\Phi^{(2)}$. ($\delta n = n - \bar{n}$ denotes the deviation from the equilibrium value \bar{n} .) $\delta\Gamma[\delta n]$ determines both static and dynamic properties of the Fermi liquid. In particular, it yields the quantum Boltzmann equation satisfied by $n_{\mathbf{k}\sigma}(\mathbf{r}, \tau)$. In the static case, the Wigner distribution $\{n_{\mathbf{k}\sigma}(\mathbf{r}, \tau)\}$ re-

duces to the quasi-particle distribution function $\{n_{\mathbf{k}\sigma}\}$, and $\delta\Gamma[\delta n] = \delta E[\delta n] - \mu\delta N - T\delta S[\delta n]$ where $\delta N[\delta n]$ and $\delta S[\delta n]$ are the quasi-particle number and entropy variations induced by a change δn in the quasi-particle distribution. The functional $\delta E[\delta n]$, which gives the corresponding energy variation, is the basis of Landau's phenomenological Fermi liquid theory.

Acknowledgments

I acknowledge discussions with M. Tissier on the 2PI formalism at an early stage of this work. I am also grateful to C. Nickel and C. Bourbonnais for numerous discussions on the RG approach, and to A. Katanin for a useful comment on Ward identities.⁶⁴

APPENDIX A

In this appendix, we show that Eqs. (108) correctly reproduce the one-loop equations for the 1PI vertex $\gamma^{(4)}$ in Luttinger liquids. The flow equation of $\gamma^{(4)}$ is given by Eq. (39). To order $(\gamma^{(4)})^2$, it reduces to $\dot{\gamma}^{(4)} = -\gamma^{(4)}\dot{\Pi}\gamma^{(4)} + \dot{\Phi}^{(2)}$ where $\dot{\Phi}^{(2)}$ should be evaluated to $\mathcal{O}[(\gamma^{(4)})^2]$. This leads to

$$\begin{aligned}
\dot{\gamma}_t^C &= -B_{\text{pp}}\gamma_t^{C^2} + \dot{\Phi}_t^C \\
&= B_{\text{pp}}(-\gamma_t^{C^2} + \gamma_t^C\gamma_{\text{ch}}^L + 2\gamma_t^C\gamma_{\text{sp}}^L - \gamma_s^C\gamma_{\text{sp}}^L), \\
\dot{\gamma}_s^C &= -B_{\text{pp}}\gamma_s^{C^2} + \dot{\Phi}_s^C \\
&= B_{\text{pp}}(-\gamma_s^{C^2} + \gamma_s^C\gamma_{\text{ch}}^L - 3\gamma_t^C\gamma_{\text{sp}}^L), \\
\dot{\gamma}_{\text{ch}}^P &= 2B_{\text{ph}}\gamma_{\text{ch}}^{P^2} + \dot{\Phi}_{\text{ch}}^P \\
&= -B_{\text{pp}}(2\gamma_{\text{ch}}^{P^2} + \gamma_{\text{ch}}^P\gamma_{\text{ch}}^L + 3\gamma_{\text{sp}}^P\gamma_{\text{sp}}^L), \\
\dot{\gamma}_{\text{sp}}^P &= 2B_{\text{ph}}\gamma_{\text{sp}}^{P^2} + \dot{\Phi}_{\text{sp}}^P \\
&= -B_{\text{pp}}(\gamma_{\text{sp}}^{P^2} + \gamma_{\text{ch}}^P\gamma_{\text{sp}}^L + \gamma_{\text{sp}}^P\gamma_{\text{ch}}^L - 2\gamma_{\text{sp}}^P\gamma_{\text{sp}}^L), \\
\dot{\gamma}_{\text{ch}}^L &= \dot{\Phi}_{\text{ch}}^L \\
&= \frac{1}{2}B_{\text{pp}}\left(\frac{3}{4}\gamma_t^{C^2} + \frac{1}{4}\gamma_s^{C^2} - \gamma_{\text{ch}}^{P^2} - 3\gamma_{\text{sp}}^{P^2}\right), \\
\dot{\gamma}_{\text{sp}}^L &= \dot{\Phi}_{\text{sp}}^L \\
&= \frac{1}{2}B_{\text{pp}}\left(\frac{1}{2}\gamma_t^{C^2} - \frac{1}{2}\gamma_t^C\gamma_s^C \right. \\
&\quad \left. - 2\gamma_{\text{ch}}^P\gamma_{\text{sp}}^P + 2\gamma_{\text{sp}}^{P^2} + 4\gamma_{\text{sp}}^{L^2}\right), \tag{A1}
\end{aligned}$$

where we have used $B_{\text{pp}} = -B_{\text{ph}}$. γ^C , γ^P and γ^L are defined similarly to Φ^C , Φ^P and Φ^L [Eqs. (106)]. Note that $\gamma^{(4)}\dot{\Pi}\gamma^{(4)}$ vanishes in the Landau channel as it does not produce any logarithmic term. Eqs. (A1) can be simplified by using the crossing symmetries

$$\begin{aligned}
\gamma_{\text{ph},\sigma_1\sigma_2\sigma_3\sigma_4}^{(4)r\bar{r}\bar{r}} &= -\gamma_{\text{pp},\sigma_1\sigma_3\sigma_2\sigma_4}^{(4)r\bar{r}\bar{r}} = \gamma_{\text{pp},\sigma_1\sigma_3\sigma_4\sigma_2}^{(4)r\bar{r}\bar{r}} \\
&= -\gamma_{\text{ph},\sigma_1\sigma_4\sigma_3\sigma_2}^{(4)r\bar{r}\bar{r}}, \tag{A2}
\end{aligned}$$

which lead to

$$\begin{aligned}
\gamma_{\text{ch}}^L &= \frac{3}{4}\gamma_t^C + \frac{1}{4}\gamma_s^C = -\frac{1}{2}\gamma_{\text{ch}}^P - \frac{3}{2}\gamma_{\text{sp}}^P, \\
\gamma_{\text{sp}}^L &= \frac{1}{4}\gamma_t^C - \frac{1}{4}\gamma_s^C = -\frac{1}{2}\gamma_{\text{ch}}^P + \frac{1}{2}\gamma_{\text{sp}}^P. \tag{A3}
\end{aligned}$$

From Eqs. (A1,A3), we finally deduce

$$\begin{aligned}
\dot{\gamma}_t^C &= \frac{1}{4}B_{\text{pp}}(\gamma_t^C - \gamma_s^C)^2, \\
\dot{\gamma}_s^C &= -\frac{3}{4}B_{\text{pp}}(\gamma_t^C - \gamma_s^C)^2, \\
\dot{\gamma}_{\text{ch}}^P &= -\frac{3}{2}B_{\text{pp}}(\gamma_{\text{ch}}^P - \gamma_{\text{sp}}^P)^2, \\
\dot{\gamma}_{\text{sp}}^P &= \frac{1}{2}B_{\text{pp}}(\gamma_{\text{ch}}^P - \gamma_{\text{sp}}^P)^2, \\
\dot{\gamma}_{\text{ch}}^L &= 0, \\
\dot{\gamma}_{\text{sp}}^L &= 4B_{\text{pp}}\gamma_{\text{sp}}^{L^2}, \tag{A4}
\end{aligned}$$

with the initial value $\gamma^{(4)}|_{\Lambda_0} = \Phi^{(2)}|_{\Lambda_0}$ given by Eqs. (112). Alternatively, using the parameterization (112), one can rewrite Eqs. (A4) as two flow equations for g_1 and g_2 ,

$$\begin{aligned}
\dot{g}_1 &= -2B_{\text{pp}}g_1^2, \\
2\dot{g}_2 - \dot{g}_1 &= 0. \tag{A5}
\end{aligned}$$

Eqs. (A5) are the usual one-loop RG equations for a 1D system.¹²

¹ J. M. Luttinger and J. C. Ward, Phys. Rev. **118**, 1417 (1960).

² G. Baym and L. P. Kadanoff, Phys. Rev. **124**, 287 (1961).

³ G. Baym, Phys. Rev. **127**, 1391 (1962).

⁴ C. De Dominicis and P. C. Martin, J. Math. Phys. **5**, 14 and 31 (1964).

⁵ The 2PI formalism has been generalized to relativistic field theories by J. M. Cornwall, R. Jackiw and E. Tomboulis, Phys. Rev. D **10**, 2428 (1974).

⁶ In bosonic systems, the functional Γ depends also on the expectation value of the bosonic field.

⁷ Φ -derivable approximations satisfy conservation laws and

- Ward identities in fermion systems.³ More generally, expectation values of the Noether currents corresponding to global symmetries are conserved, but Ward identities for the self-energy and higher-order vertex functions can be violated, e.g. in bosonic systems with broken gauge invariance (see Ref. 48).
- ⁸ N. E. Bickers, D. J. Scalapino, and S. R. White, Phys. Rev. Lett. **62**, 961 (1989).
- ⁹ N. E. Bickers and D. J. Scalapino, Annals of Physics **193**, 206 (1989).
- ¹⁰ Y. Vilk and A.-M. S. Tremblay, J. Phys. I **7**, 1309 (1997).
- ¹¹ C. Wetterich, cond-mat/0208361.
- ¹² C. Bourbonnais, in *Les Houches, Session LVI (1991), Strongly interacting fermions and high- T_c superconductivity*, edited by B. Douçot and J. Zinn-Justin (Elsevier Science, Amsterdam, 1995), p. 307.
- ¹³ R. Duprat and C. Bourbonnais, Eur. Phys. J. B **21**, 219 (2001).
- ¹⁴ C. Bourbonnais and R. Duprat, J. Phys. IV France **114**, 3 (2004).
- ¹⁵ J. C. Nickel, R. Duprat, C. Bourbonnais, and N. Dupuis, cond-mat/0502614.
- ¹⁶ J. C. Nickel, R. Duprat, C. Bourbonnais, and N. Dupuis, in preparation.
- ¹⁷ Y. Fuseya and Y. Suzumura, J. Phys. Soc. Jpn. **74**, 1264 (2005).
- ¹⁸ G. Abramovici, J. C. Nickel, and M. Heritier, Phys. Rev. B **72**, 045120 (2005).
- ¹⁹ K.-M. Tam, S.-W. Tsai, and D. K. Campbell, cond-mat/0505396.
- ²⁰ D. Zanchi and H. J. Schulz, Europhys. Lett. **44**, 235 (1998).
- ²¹ D. Zanchi and H. J. Schulz, Phys. Rev. B **61**, 13609 (2000).
- ²² C. J. Halboth and W. Metzner, Phys. Rev. B **61**, 7364 (2000).
- ²³ C. Honerkamp, M. Salmhofer, N. Furukawa, and T. M. Rice, Phys. Rev. B **63**, 035109 (2001).
- ²⁴ C. Honerkamp and M. Salmhofer, Phys. Rev. B **64**, 184516 (2001).
- ²⁵ M. Salmhofer and C. Honerkamp, Prog. Theor. Phys. **105**, 1 (2001).
- ²⁶ C. Honerkamp, M. Salmhofer, and T. M. Rice, Eur. Phys. J. B **27**, 127 (2002).
- ²⁷ C. Honerkamp, D. Rohe, S. Andergassen, and T. Enss, Phys. Rev. B **70**, 235115 (2004).
- ²⁸ M. Salmhofer, C. Honerkamp, W. Metzner, and O. Lauscher, Prog. Theor. Phys. **112**, 943 (2005).
- ²⁹ P. Kopietz and T. Busche, Phys. Rev. B **64**, 155101 (2001).
- ³⁰ T. Busche, L. Bartosch, and P. Kopietz, J. Phys.: Cond. Matt. **14**, 8513 (2002).
- ³¹ S. Ledowski and P. Kopietz, J. Phys.: Cond. Matt. **15**, 4779 (2003).
- ³² F. Schütz, L. Bartosch, and P. Kopietz, Phys. Rev. B **72**, 035107 (2005).
- ³³ B. Binz, D. Baeriswyl, and B. Douçot, Eur. Phys. J. B **25**, 69 (2002).
- ³⁴ B. Binz, D. Baeriswyl, and B. Douçot, Ann. Phys. **12**, 704 (2003).
- ³⁵ A. A. Katanin and A. P. Kampf, Phys. Rev. B **68**, 195101 (2003).
- ³⁶ A. A. Katanin and A. P. Kampf, Phys. Rev. Lett. **93**, 106406 (2004).
- ³⁷ A. Schwenk, B. Friman, and G. E. Brown, Nucl. Phys. A **713**, 191 (2003).
- ³⁸ T. Baier, E. Bick, and C. Wetterich, Phys. Rev. B **70**, 125111 (2004).
- ³⁹ T. Baier, E. Bick, and C. Wetterich, Phys. Lett. B **605**, 144 (2005).
- ⁴⁰ H. Freire, E. Corrêa, and A. Ferraz, Phys. Rev. B **71**, 165113 (2005).
- ⁴¹ The IPI RG scheme was first introduced in quantum field theory and statistical physics. For a review, see J. Berges, N. Tetradis, and C. Wetterich, Phys. Rep. **363**, 223 (1993).
- ⁴² Y. Fuseya, H. Kohno, and K. Miyake, J. Phys. Soc. Jpn. **74**, 722 (2005).
- ⁴³ W. Metzner, J. Reiss, and D. Rohe, cond-mat/0509412.
- ⁴⁴ T. M. Morris, Int. J. Mod. Phys. A **9**, 2411 (1994).
- ⁴⁵ R. Shankar, Rev. Mod. Phys. **66**, 129 (1994).
- ⁴⁶ H. Van Hees and J. Knoll, Phys. Rev. D **65**, 105005 (2002).
- ⁴⁷ H. Van Hees and J. Knoll, Phys. Rev. D **65**, 025010 (2002).
- ⁴⁸ H. Van Hees and J. Knoll, Phys. Rev. D **66**, 025028 (2002).
- ⁴⁹ J. P. Blaizot, E. Iancu, and U. Reinosa, Nucl. Phys. A **736**, 149 (2004).
- ⁵⁰ Note that due to the antisymmetry of G and J , the chain rule for derivation includes additional $\frac{1}{2}$ factors, e.g. $\frac{\delta W[J]}{\delta G_{\gamma}} = \frac{1}{2} \sum_{\gamma'} \frac{\delta J_{\gamma'}}{\delta G_{\gamma}} \frac{\delta W[J]}{\delta J_{\gamma'}}$. For the same reason, we have $\frac{\delta G_{\gamma_1}}{\delta G_{\gamma_2}} = \frac{\delta J_{\gamma_1}}{\delta J_{\gamma_2}} = I_{\gamma_1 \gamma_2}$ where I is the unit matrix defined in Eq. (12).
- ⁵¹ R. Haussmann, *Self-consistent quantum field theory and bosonization for strongly correlated electron systems* (Springer, New York, 1999).
- ⁵² Note that our derivation of the universality of the LW functional is non perturbative as it does not rely on any diagrammatic expansion. For a related discussion, see M. Potthoff, cond-mat/0406671.
- ⁵³ The functionals $F[\Sigma]$ and $\Gamma[\Sigma]$ have been introduced in the context of the self-energy functional approach by M. Potthoff, Eur. Phys. J. B **32**, 429 (2003).
- ⁵⁴ Eq. (92) follows from (82) and (85). To avoid ambiguities due to factors $\Theta(0)$, we use $\partial_{\Lambda} = \partial_{\Lambda}|_{\Delta} + \hat{\Delta} \partial_{\Delta}$, and carry out the sums over momentum before applying $\partial_{\Lambda}|_{\Delta}$. The same trick is used to calculate the ground state condensation energy in Sec. III B 1.
- ⁵⁵ P. W. Anderson, Phys. Rev. **112**, 1900 (1958).
- ⁵⁶ N. N. Bogoliubov, Sov. Phys. JETP **34**, 41 and 51 (1958).
- ⁵⁷ N. Dupuis, unpublished.
- ⁵⁸ A pairing instability in a high angular momentum channel can occur when the normal phase remains stable down to extremely low temperatures (Kohn-Luttinger effect). Such an instability would however not be experimentally observable.
- ⁵⁹ T. Vuletic, P. Auban-Senzier, C. Pasquier, S. Tomic, D. Jérôme, M. Héritier, and K. Bechgaard, Eur. Phys. J. B **25**, 319 (2002).
- ⁶⁰ I. J. Lee, S. E. Brown, W. Yu, M. J. Naughton, and P. M. Chaikin, Phys. Rev. Lett. **94**, 197001 (2005).
- ⁶¹ J. P. Pouget and S. Ravy, J. Phys. I (France) **6**, 1501 (1996).
- ⁶² S. Kagoshima, Y. Saso, M. Maesato, R. Kondo, and T. Hasegawa, Sol. State. Comm. **110**, 479 (1999).
- ⁶³ N. Dupuis, Int. J. Mod. Phys. B **14**, 379 (2000).
- ⁶⁴ A. A. Katanin, Phys. Rev. B **70**, 115109 (2004).